TRIBHUVAN UNIVERSITY

INSTITUTE OF ENGINEERING

PULCHOWK CAMPUS

THESIS NO. PUL080MSGtE017

Influence of Steep Topography on Rock Burst Mechanism and Its Prevention "A Case Study of Rolwaling Khola Hydropower Project (22 MW)"

by

Saransh Mool

A THESIS

SUBMITTED TO THE DEPARTMENT OF CIVIL ENGINEERING

IN PARTIAL FULFILLMENT OF THE REQUIREMENTS FOR THE

DEGREE OF MASTER OF SCIENCE IN

GEOTECHNICAL ENGINEERING

DEPARTMENT OF CIVIL ENGINEERING

LALITPUR, NEPAL

APRIL, 2026

COPYRIGHT

TRIBHUVAN UNIVERSITY

INSTITUTE OF ENGINEERING

PULCHOWK CAMPUS

DEPARTMENT OF CIVIL ENGINEERING

The thesis titled "Influence of Steep Topography on Rock Burst Mechanism and Its Prevention: A Case Study of Rolwaling Khola Hydropower Project (22MW)" prepared and submitted by Saransh Mool in partial fulfilment of the requirements for the degree of Master of Science (M. Sc.) in Geotechnical Engineering has been examined by us and is accepted for the award of M. Sc. In Geotechnical Engineering by Tribhuvan University.

The undersigned certify that they have read, and recommended to the Institute of Engineering for acceptance, a thesis report entitled "Influence of Steep Topography on Rock burst Mechanism and Its Prevention: A Case Study of Rolwaling Khola Hydropower Project (22MW)" submitted by Saransh Mool in partial fulfillment of the requirements for the degree of Master in Geotechnical Engineering

Supervisor:
Assist. Prof. Santosh Kumar Yadav
Department of Civil Engineering
IOE, Pulchowk Campus

External Examiner:
Dr. Gyanendra Lal Shrestha
Immediate Past President
Nepal Tunneling Association

Program Coordinator:
Assist. Prof. Bhim Kumar Dahal
M.Sc. in Geotechnical Engineering
Department of Civil Engineering
IOE, Pulchowk Campus

Date: April 27, 2026

DECLARATION

I hereby declare that this study, titled "**Influence of Steep Topography on Rock Burst Mechanism and Its Prevention: A Case Study of Rolwaling Khola Hydropower Project (22MW)**" is based on my original research work. Related works on the topic by other researchers have been duly acknowledged. I owe all the liabilities relating to the accuracy and authenticity of the data and any other information included hereunder.

Saransh Mool

080/MSGtE/017

MSc in Geotechnical Engineering

Date: April 27, 2026

ACKNOWLEDGEMENTS

I would like to express my sincere gratitude towards my supervisor, Dr. Santosh Kumar Yadav, for his invaluable guidance, constant support and encouragement throughout the project. The suggestions provided helped me to develop the research work to the next level. His expertise and encouragement were essential to this study.

I would wholeheartedly like to thank my external examiner, Prof. Dr. Gyanendra Lal Shrestha for his valuable suggestions and guidance for the thesis work. I am also incredibly grateful to Associate Professor Indra Prasad Acharya, Assistant Professor Bhim Kumar Dahal, and Assistant Professor Ram Chandra Tiwari, as well as the entire Geotechnical Engineering Department at Pulchowk Campus. Their relentless support and the opportunities they have afforded me have played a pivotal role in expanding my perspectives and enhancing my academic journey.

I extend my heartfelt gratitude to Geotechnical Er. Saphal Lamichhane, Hydropower Er. Agraj Khakurel and Geologist Chitra Bikram Tandon for their steadfast guidance, dedicated support, and invaluable contributions throughout this research. Special thanks go to Upper Tamakoshi Hydropower Limited for kindly supplying the critical data essential to this study.

Lastly, I am sincerely grateful to my family and friends for their unwavering inspiration and invaluable support throughout my studies. Additionally, I extend my thanks to all the individuals who directly or indirectly contributed to this endeavor.

Saransh Mool

080/MSGtE/017

MSc in Geotechnical Engineering

April, 2026

ABSTRACT

A rock burst is a violent failure in hard, brittle rocks caused by rapid stress redistribution after underground excavation. This study on the 22 MW Rolwaling Khola Hydropower Project shows that steep topography significantly increases rock burst potential in the headrace tunnel even in low overburden. Numerical analysis of different valley conditions indicates that both deviatoric and tangential stresses rise from non-valley to longitudinal and cross-sectional valley settings, with the cross-sectional valley producing the highest stresses (about 64–66 MPa tangential stress and 18.5–19.2 MPa deviatoric stresses). These stresses can approach rock mass strength even at low overburden, indicating that steep terrain creates unexpectedly high-risk zones for rock bursts.This study also analyzes the concept of mitigating rock bursts based on the magnitude and direction of the stress caused by steep topography, with attention given to two preventative strategies: the stress relief holes and the rock support systems. Smaller, closely spaced peripheral holes reduce stress more effectively than larger, widely spaced ones by promoting uniform stress dissipation and better controlling localized stress concentration. Moreover, the enhanced support system (15 cm wire mesh shotcrete, 1.5 m spacing between bolts and 2.7 m length of bolts) contributes to the stability of the tunnels because it will improve the safety factor of the shotcrete and reduce the yielding of the bolts in the high-stress environment.

Keywords: Rock Burst, Tangential Stress, Deviatoric Stress, Rocscience, Phase2, Steep Valley, Stress Relief Holes

TABLE OF CONTENTS

LIST OF FIGURES

LIST OF TABLES

ABBREVIATIONS AND ACRONYMS

γ	Unit Weight
2D	Two Dimensional
CVM	Cross-Sectional Valley Model
D/B	Drilling and Blasting
DPR	Drilling Pressure Relief
FEM	Finite Element Modelling
GSI	Geological Strength Index
HRT	Headrace Tunnel
LVM	Longitudinal Valley Model
MN	Mega Newtons
MPA	Mega Pascals
MW	Mega Watts
RBI	Rock Burst Intensity
RMR	Rock Mass Rating
RS	Rocscience
SRH	Stress Relief Holes
TS	Tangential Stress
UCS	Unconfined Compressive Strength

1 INTRODUCTION

1.1 Background

Tunnelling plays an important role in the construction of underground projects, especially in hydropower engineering, where long head-race tunnels are typically constructed to transport water from the intake to the powerhouse. Mountainous sites, like the Himalayan region, pose special challenges in tunnel construction because of the variable geological formations, varying ground conditions and overburden pressure. This can result in a range of technical problems and hazards during tunnelling.

The most common issues in tunnel construction are water inrush, rock fall, squeezing ground, overbreak, faults and settlements. One of the most violent, unpredictable, and risky of these is Rock Burst: explosive failures of rock around underground excavations, due to very high stress concentrations, such as in deep mining of hard, brittle rocks (Hoek, 2001). Rock bursts are explosive failures of rocks surrounding underground excavations, which occur due to extreme stress concentrations around these (Hoek, 2001). They are typically observed in deep mining for hard, brittle rock, but have also been reported in tunnels, shafts and other long-term underground structures in the same type of rocks, forming the focus of the current thesis. In tunnels, rock bursts can be a serious safety risk for workers and assets, and impact on tunnelling performance and contracts. With the current trend towards deeper and more challenging geological conditions, reports of tunnel rock bursts have been growing. The processes, triggers and impacts of these events are detailed in Chapter 2.

While rock bursts have been reported all over the world, they have often been studied independently. Many studies have been conducted on a site-by-site basis, with little consideration given to other sites. In addition, a substantial body of rock mechanics research over the last few decades in countries such as Russia, Japan, and China have been relatively inaccessible to the English-speaking community. Consequently, the case histories and references used in this thesis are concentrated mainly on projects in the United States, Canada, Europe, and South Africa, except where international collaborations provide broader coverage.

When excavations are subjected to high in situ stresses, failure modes such as slabbing, spalling, and zonal disintegration often occur (Dowding & Andersson, 1986). Among these, Rock bursts: violent failures associated with sudden energy

release in hard and brittle rocks are particularly severe. Although likely present since early underground mining, documented rock burst incidents date back to the 18th century. The earliest reported case was in a British tin mine in 1738, with another documented incident at a coal mine in Stafford in 1938. A particularly intense rock burst event in 1900 at the Golden Horn area in India caused destruction even at the surface level. Similar occurrences have been reported in mines and tunnels across regions including Africa, Australia, Canada, China, Chile, Korea, Norway, Russia, Sweden, and the United States (Fukui et al., 2004).

Figure 1.1: Rock burst (Source: Google)

1.2 Research Gaps and Problem Statement

The selected case study is the Rolwaling Khola Hydropower Project located in the Lamabagar area of Dolakha District, Bagmati Province, central Nepal. It is a run-of-river scheme on the Rolwaling Khola that will divert flow through a headrace tunnel to the Tamakoshi system and contribute additional dry-season energy to the Upper Tamakoshi cascade. The underground works include long headrace and access tunnels, surge arrangements, and powerhouse caverns excavated at substantial depth beneath steep valley flanks.

The project is located in the Higher Himalayan Crystalline belt, with high grade metamorphic rocks (banded gneiss, schist and associated crystalline rocks) extensively exposed. Banded gneiss is the main rock type along the tunnel route,

generally medium to coarse-grained with alternating bands of quartz–feldspar-biotite and local garnet bearing rocks. The rock mass is intersected by several joint sets and shear zones, and is affected by regional-scale thrusts and folds typical of the central Himalaya. These structures, combined with the large overburden of the narrow glacial valley, produce a highly anisotropic and elevated in-situ stress field, which is favourable for rock burst development.

Despite being planned and designed using standard rock mass classification and empirical support methods, the Rolwaling hydropower tunnels have experienced rock burst-type damage in banded gneiss sections. These events/assessments indicate that conventional use of indices such as RMR, Q and GSI, together with basic checks on stress ratio (σ_θ/UCS), does not adequately capture the combined effects of high in-situ stress, rock brittleness and geological structures in the Rolwaling setting. The spatial distribution, timing, and intensity of rock bursts around the tunnel cannot yet be predicted with sufficient reliability for safe and efficient construction. Existing support concepts may not be optimized for energy absorption and controlled damage in burst-prone banded gneiss.

During the construction of the Rolwaling Hydropower Project, problems were encountered during excavation due to hard, brittle rocks and rock bursting. The major problems that could occur due to rock bursts are as follows:

- **Failure of Rock Supports**: Rock bursts can damage rock supports such as shotcrete, rock bolts and steel linings, causing loss of support and stability.
- **Spalling, Rock Falls, and Tunnel Stability**: Bursts lead to spalling and rock falls, threatening tunnel stability.
- **Injury and Death**: Safety hazards from falling rocks from bursts can cause injury or death.
- **Damage to Equipment**: Rock bursts can damage excavation and blasting equipment, leading to delays.
- **Delays and Cost Overruns**: Rock bursts severely delay the excavation work, leading to a longer construction period and cost overruns.

Figure 1.2: Rock burst (Rolwaling Khola Hydropower Project)

1.3 Objectives

The project aims to study the rock burst in the headrace tunnel of Rolwaling Khola HPP and how to mitigate this. The study mainly focuses on the following objectives:

- To identify the geological environment, structure and rock mass properties (UCS, E, GSI, RMR, Q, joint sets) of banded gneiss along the tunnel.
- To understand the causes and influencing factors of rock burst in the Rolwaling tunnels and to predict the occurrence and severity of rock burst hazard based on empirical methods and stress criteria.
- To build and calibrate numerical models (e.g., 2D/3D FEM) to predict the stress field, stress redistribution and brittle failure/energy release associated with the excavation.
- To verify the model (and empirical) assessment results against rock burst incidents (location, timing, damage) and to assess the effectiveness and limits of the adopted assessment approach.
- To investigate and recommend effective rock burst control measures (such as excavation sequence, stress relief drilling, yielding/energy absorbing support) and their likely performance in Rolwaling.
- To develop a practical assessment and control strategy for rock bursts for Rolwaling and other Himalayan hydropower tunnels.

1.4 Significance

The study is significant for the safety, design and future of tunnels in the Himalaya. It can be seen in the following points: The research helps to determine where and why rock bursts may occur in the Rolwaling tunnel, enabling risk zoning rather than blanket assumptions. Significances of the study are as follows:

- **Enhanced safety of rock burst-prone tunnels:** Determines where potential risk zones exist on the Rolwaling tunnel, allowing targeted safety measures to be put in place, such as monitoring, exclusion zones and specialist support systems.
- **Efficient and economical support design**: Informs the choice of support systems, avoiding under-design of support systems to ensure safety, and unnecessary costs due to over-design of support systems.
- **Improved knowledge of the Himalayan banded gneiss:** Provides evidence of banded gneiss behaviour under high stress, which can be applied to other tunnelling projects in the Himalayan region.
- **Testing and calibrating rock burst criteria:** Validates and calibrates rock burst criteria using local data to better understand their use in Himalayan tunnels.
- **Case study and modelling legacy for future studies and hydropower tunnels**: Provides a case study and model baseline for improving design, enabling future research and development of national hydropower tunnels.

1.5 Limitations

There is a lack of data on geology, stress and monitoring in this project, which limits the detail and accuracy of the analysis. The limitations are:

- The Himalayan rocks are highly heterogeneous, fractured and faulted, and the results are difficult to apply to other regions.
- There is often a lack of sophisticated monitoring equipment and funds to support detailed field studies and precise simulations.

- Type of terrain may restrict the deployment and maintenance of high-tech monitoring systems, which can limit real-time monitoring and analysis for detecting potential rock burst precursors.
- Operational challenges, including access restrictions, challenges in transporting equipment and materials, and limited work space, can impact data acquisition and mitigation efforts. The study assumes isotropic rock mass properties, which may influence results to some degree; incorporating rock mass anisotropy could enhance accuracy.
- This analysis uses 2D finite element modelling; future work could employ 3D finite element models for greater precision.
- Valleys were developed as two separate configurations (longitudinal and cross-sectional); advanced 3D software could integrate them into a combined model to better represent actual site conditions.
- Discontinuities and groundwater conditions are not considered in the analysis; including these would improve the reliability.
- Only UCS values from the laboratory test of the rock sample were available and used in the numerical analysis; conducting laboratory tests for additional parameters (e.g., Young's modulus, Poisson's ratio) could refine the outcomes.

2 LITERATURE REVIEW

2.1 History of Rock Burst in Hydropower Tunnel

Rock bursts have been a major issue in several large new hydropower projects, especially in high-stress, tectonically active areas such as the Himalayas and southwest China. A notable example is the Parbati II Hydroelectric Power Project in India, where the headrace tunnel suffered from numerous rock bursts, particularly after the 7.5 km chainage in the Manikaran quartzite section (Zhuang et al., 2022). The catastrophic failures occurred almost every time blasting was carried out, injuring workers and slow tunnel advancement down to 10 meters per month. Construction team's countermeasure by installing steel fiber shotcrete and rock bolts in the tunnel, and for the TBM-excavated part of the tunnel, steel ring beams and steel netting were applied to manage rock splitting and falls.

Another notable case is the Neelum-Jhelum Hydropower Project, Pakistan. This project has experienced extremely severe rock burst events due to exceptionally high horizontal stresses and intricate geological settings, especially in the TBM-excavated twin tunnels through sedimentary sandstone formations. On May 31, 2015, a severe rock burst caused a tunnel collapse, damage to support structures, injuries, human lives, and damaged TBM, delaying the work for more than six months. Stress-relieving measures such as vertical and horizontal holes and a pilot tunnel that used the drill and blast method were implemented, but only had limited impact in the most critical areas (Zhuang et al., 2022)

Another example outside of the Himalaya is the Jinping II Hydropower Station in southwest China, which also encountered very severe rock bursts during the deep tunnel excavation Notably, during the construction of the drainage tunnel and headrace tunnel No. 4, several rock bursts led to fatalities, injuries, and significant equipment damage. These events were attributed to the combination of deep overburden, high in-situ stress, and brittle marble lithology (Zhuang et al., 2022). Detailed field investigations and numerical modelling have provided valuable insights into the mechanisms and progression of rock burst damage in these deep tunnels, informing the development of more effective rock burst- resistant support measures.

In Nepal's hydropower sector, the Nilgiri Khola Hydropower project (38 MW) in Myagdi district emerges as a prominent example of rock burst challenges in deep underground excavations involving hard gneiss and schist under overburden depths exceeding 500-1000 m, which have amplified risks during head-race tunnel construction, particularly evident around the project's 2022 breakthrough milestone. These strain-type bursts, induced by stress concentrations at the excavation boundary, highlight Nepal's susceptibility in comparable high-stress Himalayan tunneling projects

2.2 Classification of Rock Burst

To predict rock bursts, it is necessary to first understand the definitions, classifications and mechanisms of rock bursts. Rock bursts are typically defined as sudden and violent rock failures caused by the rapid release of stored elastic strain energy, resulting from changes in the in-situ stress, especially the increase in tangential stress (σ_θ) and the decrease in radial stress (σ_r)) (Zhou et al., 2024). Historical definitions of rock bursts have focused on different aspects of the phenomenon: Terzaghi (1946) described sudden detachments of rocks under stress, while Cook (1963) and Obert and Duvall (1967) pointed out the explosive nature of the failures due to stresses exceeding the rock strength. More recent perspectives emphasise the release of energy and rock mass ejection during mining (Dietz et al., 2018). These definitions continually revolve around the influence of in situ stresses and energy release in causing rock bursts.

Over time, several classifications of rock bursts have emerged to explain their mechanisms and effects. (Ortlepp & Stacey, 1994) classified rock bursts as strain burst, buckling, ejection and arch collapse. Strain bursts usually occur in massive and intact rocks under moderate stress, with the ejection of sharp-edged fragments (Singh, 1987). Buckling usually occurs at the edge of excavations in layered or massive rocks, and can be caused by stored energy or dynamic loads such as blasting (Singh, 1987). Ejection and arch collapse bursts are sudden releases of rock blocks affected by geological structures. In addition, other researchers have proposed different classifications, including Hedley's (1992) inherent, induced and fault slip bursts; Kaiser's (1996) self-initiated and remotely

triggered bursts; and Tang's (2000) mixed strain burst-fault slip mechanism. In recent years, Li et al. (2017b) developed a systematic geomechanical classification, which considers six different failure mechanisms, combining both stress and structural effects.

Rock burst classifications aim to determine the failure mechanisms and potential risks in underground construction. The initial classifications, such as that of Colson (1950) based on origin, were refined to include failure patterns, seismicity and rock burst intensity (Ortlepp & Stacey, 1994). Classification criteria include volume change of the rock mass, deformation of the tunnel wall and intensity of ejection (Ortlepp & Stacey, 1994). A crucial difference lies between the source and the location of damage. If these are the same (such as buckling), the rock burst is initiated at the energy source. By contrast, remotely triggered rock bursts, such as shear rock bursts, might occur well away from the energy source, such as an earthquake or blasting area. These differences highlight the need for a refined classification system to inform risk management and design strategies for deep underground workings.

The key differences between Type I and Type II rock bursts are their source, triggering mechanism and effects on underground structures. Type I rock bursts take place near the excavation wall and are triggered by high tangential stresses during tunnelling, which often causes local failure at the tunnel wall (strain burst behavior) and usually occurs within 100 m of the face. On the other hand, Type II rock bursts are caused by slip along tectonically stressed, pre-existing faults, and can occur at some distance from the excavation (exposure may just trigger the event). The seismic waves are then transferred to the tunnel, resulting in vibration damage. Type I events are intimately connected with excavation and are typically smaller (like tunnel-induced seismicity), whereas Type II events can be larger (like natural earthquakes) and are not obviously related to excavation.

2.3 Factors influencing the severity of Rock Bursts

The design of underground excavations should consider the in-situ stress. It's a fact that rock bursts are more frequent and violent with increasing depth, as the

overburden increases, causing higher levels of stress in the rock mass. Moreover, the competency of the rock mass also tends to increase with depth, which increases its ability to store strain energy. But the occurrence of rock bursts cannot be completely associated with depth. For instance, minor rock bursts have occurred in shallow tunnels in Norway and major bursts in shallow mines (depths of less than 300 meters). As such, the stress ratio factor ($k = \sigma_h/\sigma_v$) for deep tunnels or mines (0.5) cannot be used in general. In some deep mines, residual stresses have also been measured that result in k ratios of up to 1.8 (Durrheim), suggesting that other conditions exist which require direct stress measurements.

Shallow rock bursts are mainly caused by high horizontal stresses, which are often tectonic stresses acting sub-parallel to the surface. For example, horizontal stresses of several MN/m^2 have been measured in a granite gneiss quarry at a depth of 20 meters in Lithonia, Georgia. The local Lithonia Gneiss or Migmatite is a high-grade metamorphic rock partially melted by intense heat, and is considered to be between a metamorphic and an igneous rock. When it comes to deep mines, the occurrence of rock bursts is usually first encountered at depths of 700 meters and increases with depth at depths over 1000 meters. However, some mines have operated at depths greater than 2000 meters without rock bursts, indicating that other factors play an important role in the occurrence of rock bursts. This shows the need to consider various geological and stress factors in relation to rock bursts. The various factors influencing the rock burst are as follows:

- **High in situ stress and stress concentration:** Rock bursts primarily occur in a high-stress environment where the stress is redistributed and relaxed around the tunnel and exceeds the rock strength, failing.
- **Rock properties (strength, brittleness, energy storage)**: High-strength, stiff, and brittle rocks (e.g., gneiss, granite) can accumulate significant elastic energy and release it abruptly, thus being highly susceptible to violent rock bursts once the peak strength is reached.
- **Geological and structural conditions:** Geological structures such as faults, joints, folds and contacts affect the stress build-up and release, determining whether the failure happens locally (Type I) or by fault slip and seismic waves (Type II).

- **Excavation and operational effects**: Stress is disturbed by tunnel excavation; the effects of excavation, advance rate and blasting can lead to rock bursts, particularly in a highly stressed environment.
- **Time-dependent behavior and combined effects**: Rock burst is a temporal interaction between stress, material properties and structure, where progressive energy accumulation, micro-cracking and delayed failure eventually results in sudden failure, which can be influenced by instantaneous events and time-dependent processes.

2.4 Prediction of Rock Burst

Rock burst prediction is an important consideration in underground construction and mining, as these catastrophic events can be dangerous. A number of prediction approaches have been developed and improved since the 1960s through experimentation, numerical modelling and artificial intelligence (Li et al., 2017). These approaches can broadly be categorized as regional, local and current prediction. Regional prediction considers the geological conditions such as rock type, mechanics and geological structures. Local prediction considers local areas of the rock mass that are susceptible due to factors including depth and previous mining (Gong & Li, 2007). But the present prediction is based on real-time monitoring to identify stress concentration during underground excavation (Gong & Li, 2007). Empirical prediction methods are also widely used, and are based on either stress or energy criteria, with rock burst classified into four categories (none, light, medium or severe) based on the damage and energy release (Cook, 1963).

In particular, stress-based methods are the most common because they are simple and effective, especially in deep mines (Gong & Li, 2007). These approaches employ geomechanical parameters and stresses to predict rock burst potential. For example, drill cores are often used in observational studies. In particular, core discing (breaking of rock core into discs) can reveal high in situ stress and instability. This is due to the sudden release of stress during drilling operations, particularly in brittle rocks and may indicate areas where rock burst is more likely to occur (Gong & Li, 2007). Identifying such overstressed areas is essential for

implementing targeted safety measures and improving the overall stability of underground excavations.

a) Rock brittleness coefficient

Rock brittleness is a key property used to assess the potential intensity of rock bursts in underground excavations. Mechanically, it refers to the tendency of rock to lose strength due to weak bonding between its grains. The rock brittleness coefficient is commonly used as an indicator and is calculated as the ratio of uniaxial compressive strength (UCS) to the tensile strength of the intact rock (Akdag et al., 2017).

$Bi = \sigma_c / \sigma_t$, where σ_c is the uniaxial compressive strength of the rock and σ_t is the tensile strength of the rock. Both values are in MPa.

Table 2.1: RBI based on the brittleness coefficient (Wang & Park, 2001)

Rock Brittleness coefficient	Risk of Violent Rupture
Bi>40	No Rock burst
26.7 <Bi <40	Weak Rock burst
14.5 <Bi <26.7	Moderate Rock burst
Bi <14.5	Strong Rock burst

b) Mean stress (Tao discriminant Index) (α)

This index is based on the stress reduction factor in Q system (Barton's classification) and is defined as the ratio of the UCS of rock to the maximum principal in situ stress.

$\alpha = \sigma_c / \sigma_1$, where σ_c is the uniaxial compressive strength of the rock, and σ_1 is the maximum in situ stress.

Table 2.2: RBI based on the Tao Discriminant Index (Tao, 1988)

Mean Stress	Risk of Violent Rupture
α > 14.5	No Rock burst

$5.5 < \alpha \leq 14.5$	Weak Rock burst
$2.5 < \alpha \leq 5.5$	Moderate Rock burst
$\alpha \leq 2.5$	Strong Rock burst

c) Five Factors

Zhang and Fu (2008) proposed a five-factor criterion as a comprehensive criterion for the prediction of rock bursts. This criterion considers five involved parameters of rock burst as shown below:

Table 2.3: Five factors (Zhang & Fu, 2008)

Parameters	No Rock burst	Light Rock burst	Medium Rock burst	Strong Rock burst
σ_c/ σ_1	≤ 0.15	0.15-0.2	0.2-0.4	>0.4
σ_θ/ σ_c	≤ 0.2	0.2-0.3	0.3-0.55	>0.55
σ_c/ σ_t	<15	15-18	18-22	>22
W_{et}	<2	2-3.5	3.5-5	>5
K_u	≤ 0.55	0.55-0.60	0.6-0.8	>0.80

σ_1 = Maximum principal stress

σ_c = Uniaxial compressive strength of intact rock

σ_t = Tensile strength of intact rock

Wet = Elastic strain energy stored before failure.

K_u = Brittle deformation coefficient.

d) Tangential Stress

The tangential stress criterion is defined as the ratio of the tangential stress surrounding the excavation opening to the rock's uniaxial compressive strength (UCS), according to (Hoek & Brown, 1980a).

$Ts = \sigma_\theta / \sigma_c$

Table 2.4: TS criterion ((Wang et al. (1998) and Hoek & Brown (1980))

Tangential Stress	Risk of violent rupture
Ts<0.3	No rock burst
0.3 ≤ Ts < 0.5	Weak rock burst
0.5 ≤ Ts < 0.7	Strong rock burst
Ts ≥ 0.7	Violent rock burst

Russenes (1974) proposed another empirical approach for assessing rock burst risk, which uses the ratio of the maximum tangential stress around the rock to the rock's UCS.

Table 2.5: Rock burst prediction by Russenes (1974)

Tangential Stress	Risk of violent rupture
$\sigma_\theta / \sigma_c < 2$	No rock burst
$0.2 \leq \sigma_\theta / \sigma_c < 0.3$	Weak rock burst
$0.3 \leq \sigma_\theta / \sigma_c < 0.55$	Strong rock burst
$\sigma_\theta / \sigma_c \geq 0.55$	Violent rock burst

e) Turchaninov method

Turchanniov et al (1972) defined the Turchannov criterion to measure the rock burst intensity. This criterion is defined as

$S = \sigma_\theta + \sigma_1 / \sigma_c$

Table 2.6: Rock burst prediction by Turchaninov

Turchaninov method	Risk of violent rupture
$S < 0.3$	No rock burst
$0.3 \leq S < 0.5$	Weak rock burst
$0.5 \leq S < 0.8$	Strong rock burst
$S \geq 0.8$	Violent rock burst

2.5 Prevention of Rock Burst

Controlling the consequences of rock bursts through support measures is limited. Sometimes, it is more economical to eliminate the triggering mechanisms or reduce the severity of rock bursts. Two effective prevention methods for strain bursts include modifying the tunnel excavation shape and using destress blasting. Ground support is employed to minimize or control the severity of rock bursts.

- **Rock burst support design principles and control strategies**

Reducing rock burst risk depends largely on choosing effective advanced prediction methods. Scholars generally agree that reliable prediction requires identifying where rock bursts may occur, when they may happen, how severe they may be, and what mechanisms cause them. However, because rock masses are naturally unstable and affected by factors such as high in-situ stress, pressure relief, and strong disturbance, support design should emphasize ground control rather than depending only on uncertain predictions. For this reason, burst-resistant support systems are essential for limiting damage and maintaining operational safety, and their design principles should be considered early in a project.

Unlike conventional rock support, which mainly deals with loose rock near the surface and gravity-driven falls, support design in burst-prone ground must account for dynamic loading and large deformation. noted that tunnel damage and surrounding rock deformation under high stress are mainly caused by intense

shock waves that rapidly increase stress in the rock. (Ortlepp & Stacey, 1994) Therefore, six support principles: preventing rock burst where possible, using yielding support, paying attention to the weakest link, designing an integrated system, keeping the design simple and cost-effective, and ensuring the system remains adaptable and predictable. Together, these principles provide a practical framework for designing support in burst-prone conditions.

- **Designing and Modification of a Tunnel shape**

In elastic rock conditions, an elliptical tunnel cross-section is often considered the most favourable shape because it helps distribute stress more evenly around the excavation. However, in practice, this shape is not always easy to construct, and its advantage becomes limited when the applied stress is greater than the strength of the rock. Under such conditions, the ideal geometry alone cannot prevent failure, so the overall excavation performance depends more on how the rock responds to stress than on shape optimization alone.

From a design perspective, sharp corners are usually avoided because they create stress concentrations that may increase the likelihood of (Hoek & Brown, 1980b). However, practical observations show that corners can sometimes be beneficial in burst-prone ground. Since corners concentrate stress, spalling may begin there earlier, allowing some strain energy to be released before it accumulates excessively along the excavation surface. As noted by Kaiser and Tannant (1999), this early release of energy can reduce the chance of more sudden and severe rock burst damage.

- **Reinforce the Rock Mass**

The rock mass can be strengthened by reinforcement. Installing fully grouted rebar can increase rock strength and reduce the stress-to-strength ratio. Unfortunately, in brittle, moderately jointed rock, the effect of rebar is minor. The only damage mechanism that can be entirely prevented is low-energy strain bursting. Shotcrete combined with a dense bolting pattern has been successful in this regard.

- **Energy Release Control**

Energy release in burst-prone ground can be reduced by encouraging the rock to fail in small, controlled stages rather than all at once. When the surrounding rock undergoes progressive or incremental failure, it sheds stored strain energy gradually, which lowers the likelihood of a sudden and violent rock burst. In this sense, controlled overstressing through blasting can sometimes be used intentionally to trigger early minor failures so that the rock mass releases energy in a more manageable way.

However, not all excavation methods are equally suitable in such conditions. Tunnel boring machines and smooth blasting may leave the rock mass in a state where stress is not relieved favourably, and this can increase the chance of unstable energy accumulation around the excavation boundary. For this reason, excavation method selection should be made carefully in high-stress ground, with attention to how each method influences stress redistribution, failure mode, and the overall potential for rock burst.

- **Use of Destress Blasting**

Destress blasting is a controlled excavation technique used to lower rock burst risk by reducing the stresses around a tunnel opening. First introduced in tunnelling in the early 1950s, it is now widely used in high-stress, brittle rock conditions. The main idea is to create or enlarge a fractured zone around the tunnel so that the surrounding rock can deform and release energy more gradually instead of storing large amounts of strain energy that may be released suddenly as a rock burst.

In this method, carefully designed blasts are fired in the fractured rock immediately ahead of the tunnel face to promote slip along existing fractures and relieve the stress concentration near the excavation boundary. A typical arrangement, as described by O'Donnell (1992), uses fan-shaped blast holes that extend beyond the planned tunnel perimeter. These holes are usually grouped as face holes (F), corner holes (C), and wall holes (W). They are typically about twice as long as normal excavation holes, but explosives are loaded only in the section

beyond the regular round length. Wall holes are mainly used where two parallel tunnels are very close together, usually less than one tunnel diameter apart.

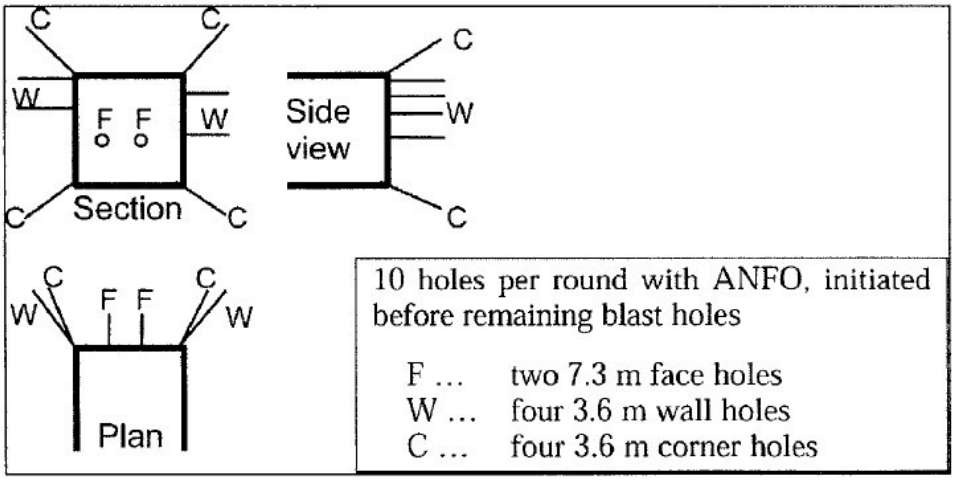

Figure 2.1: Destress blasting pattern (O'Donnell, 1992)

3 CASE STUDY AREA DESCRIPTION

3.1 Study Area

The Rolwaling Hydropower Project (Rolwaling Hydroelectric Project) is a run-of-river hydropower project in the Dolakha District of Nepal. With a capacity of around 22 MW, it is located on the Rolwaling River in the Bagmati Province. It is being developed by Upper Tamakoshi Hydropower Company Limited, which also owns the nearby 456 MW Upper Tamakoshi Hydropower Project. The project includes a subterranean powerhouse with two vertical Pelton turbines, which will use a gross head of approximately 220.5 meters and a design flow of 13.4 cubic meters per second. The powerhouse is downstream of the Upper Tamakoshi headworks and the project is anticipated to produce about 118 GWh of electricity per year.

The Rolwaling Khola Hydropower Project is located near Lamabagar in the Rolwaling Valley, in the Higher Himalayan Crystalline zone north of the Main Central Thrust. The regional geology is characterised by high grade metamorphic rocks, mainly banded gneiss, with garnet bearing gneiss, kyanite gneiss, schist, calc-schist and marble. The banded gneiss consists of light and dark bands of minerals with strong foliation, which leads to direction-dependent (anisotropic) mechanical properties. This is an important factor in determining the stability of tunnels and the potential for rock bursts.

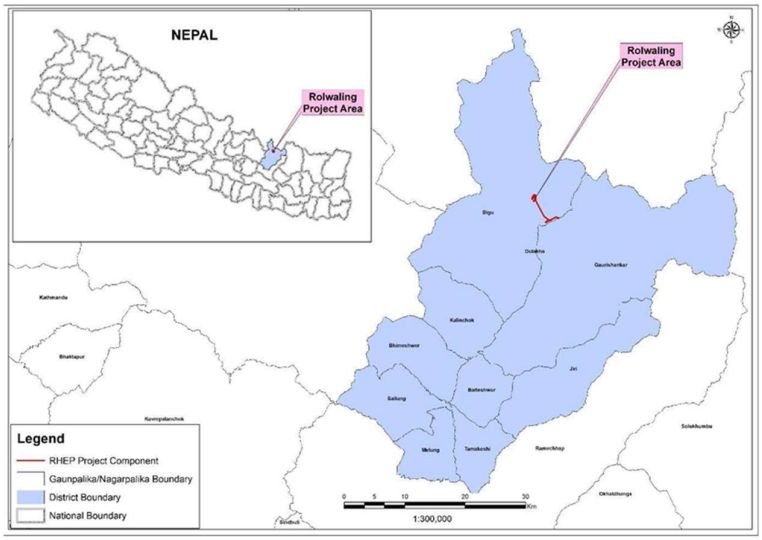

Figure 3.1: Location of Rolwaling Khola Hydropower Project (22 MW)

3.2 Regional Geology and Structural Features

The Rolwaling Khola Hydropower Project is located close to Lamabagar, in the Rolwaling Valley, in the Higher Himalayan Crystalline zone north of the Main Central Thrust. This region is comprised of high-grade metamorphic rocks, mainly banded gneiss, and includes garnet gneiss, kyanite gneiss, schist, calc-schist and marble. The banded gneiss comprises light and dark bands of minerals, which are foliated, leading to direction-dependent (anisotropic) mechanical properties. This factor is crucial in determining tunnel stability and the risk of rock bursts.

Structurally , the area is part of the Himalayan thrust system, in which large rock masses have been thrust towards the south along major thrusts like the Main Central Thrust. Successive episodes of deformation have resulted in folded beds, shear zones and locally mylonitic (pulverized) zones. On the tunnel scale, the rock mass is expected to possess multiple joint sets and foliation planes that have preferred orientations, as well as steeply-dipping cross joints, but these will vary from site to site. The steep valley slope and hard and brittle rock formations in the Rolwaling Khola Hydropower Project contribute to high and variable in-situ stresses, thus promoting the potential for rock burst, especially in the lower tunnel section.

3.3 In-Situ Stress Conditions and Depth of Overburden

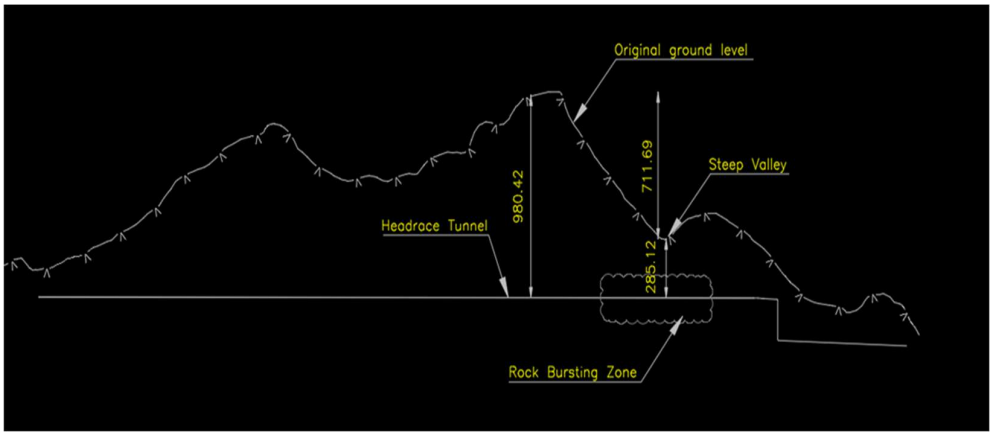

Figure 3.2: HRT of Rolwaling Khola Hydropower Project (22 MW)

The amount of rock overlying the tunnel (overburden) varies along the tunnel route. It is largest under the ridge (about 980 m), decreases towards the valley

slopes (around 711 m), and is smallest at the valley bottom (about 285 m). The vertical stress is mainly controlled by the overburden (rock mass above the tunnel) and increases with the depth. The vertical stress is greatest under the ridge. But the stability of a tunnel depends not only on vertical stress, but on the three-dimensional (3D) stress distribution.

A steep valley will significantly affect the stress distribution. While stresses are generally uniform in flat areas, a valley acts as a free surface, allowing stress to be relieved at the surface and redistributed deeper into, and around, the valley. This results in stress concentrations forming under and alongside the valley, and the principal stresses tend to rotate towards the valley slopes. This means that, despite relatively low overburden near the valley, high stress concentrations can still occur at tunnel depth. In reality, there have been cases of rock bursting both upstream and downstream of the valley within 200 m of the valley. This is due to the valley providing a stress concentration point with varying stress distribution.

The valley's steep gradient not only enhances stress magnitudes, but also changes the stress directions, aggravating the stress conditions around the tunnel following excavation. At the same time, the rock mass stores elastic strain energy, which can suddenly release during disturbances, leading to rock bursts. These findings indicate that the valley effect is important and concentrated, so such areas should be considered in the design and support of the tunnel.

3.4 Groundwater and Hydro-Mechanical Conditions

The measurements of the groundwater inflow in the headrace tunnel indicate that the water inflows into the tunnel at different rates along the tunnel axis, which is due to the heterogeneous hydrogeological conditions of the rock mass. The water flow has been measured at various locations, such as on the left and right spring lines (SPL), the crown and the center crown by collecting a certain volume of water over a specified time. The rate of flow was calculated in litres per second (L/s) and litres per minute (L/min). These data show that there are relatively higher water inflows at certain points in the tunnel, which is crucial for determining the stability of the tunnel and designing appropriate drainage and support measures. There are several high inflow locations such as 3+654.11 at the Right SPL (50 L/min),

3+722.21 at the Center Crown (33.33 L/min) and 3+960.00 at the Left SPL (60 L/min).

These elevated inflows are probably related to fractured or weaker areas, joints or other discontinuities that permit water entry into the tunnel. On the other hand, areas with low inflow, typically less than 2 L/min, correspond to relatively dry and tight rock. This variability reflects a combination of rock structure and hydrostatic pressure, particularly in areas where streams run through the valley, raising the water pressure.

The inflow measurements indicate that the water inflow is highly concentrated, corresponding to areas of rock with higher permeability and weaker structure. Higher inflows correspond to areas where additional support, grouting or drainage may be needed to ensure the stability of the tunnel. In summary, the measurements show that real-time monitoring along the tunnel is necessary in order to resolve unexpected changes in groundwater inflows, especially in areas of fracture or high pressure, which may impact on the safety of the excavation and long-term stability of the tunnel lining.

Table 3.1: Water seepage measurement at different locations

SN	Chainage	Location	Volume (L)	Time (s)	Flow (L/s)	Flow (L/min)
1	3+593.71	Left SPL	5	74	0.068	4.05
2	3+604.71	Right SPL	5	34	0.147	8.82
3	3+610.71	Right SPL	5	99	0.051	3.03
4	3+642.71	Right Crown	5	86	0.058	3.49
5	3+654.11	Right SPL	10	12	0.833	50
6	3+656.11	Right SPL	10	63	0.159	9.52
7	3+658.71	Right Crown	5	10	0.5	30

SN	Chainage	Location	Volume (L)	Time (s)	Flow (L/s)	Flow (L/min)
8	3+659.11	Right SPL	10	73	0.137	8.22
9	3+660.51	Right SPL	5	50	0.1	6
10	3+665.61	Right SPL	5	80	0.063	3.75
11	3+671.71	Center Crown	5	23	0.217	13.04
12	3+681.71	Right Crown	5	56	0.089	5.36
13	3+689.71	Right Crown	5	54	0.093	5.56
14	3+690.71	Right Crown	5	64	0.078	4.69
15	3+699.71	Right SPL	5	33	0.152	9.09
16	3+713.21	Right SPL	5	26	0.192	11.54
17	3+713.36	Left SPL	5	105	0.048	2.86
18	3+719.21	Left Crown	5	16	0.313	18.75
19	3+722.21	Center Crown	5	9	0.556	33.33
20	3+736.71	Right SPL	5	130	0.038	2.31
21	3+886.00	Right Crown	5	100	0.05	3
22	3+890.00	Right SPL	5	146	0.034	2.05
23	3+892.00	Center Crown	5	82	0.061	3.66
24	3+921.00	Left SPL	3	108	0.028	1.67

SN	Chainage	Location	Volume (L)	Time (s)	Flow (L/s)	Flow (L/min)
25	3+923.00	Right SPL	2	110	0.018	1.09
26	3+950.00	Left SPL	5	230	0.022	1.3
27	3+952.00	Right SPL	5	29	0.172	10.34
28	3+958.00	Left SPL	5	50	0.1	6
29	3+958.00	Left SPL	2.5	73	0.034	2.05
30	3+960.00	Left SPL	5	5	1	60
31	4+014.71	Left Crown	5	16	0.313	18.75
32	4+203.00	Right Crown	5	57	0.088	5.26
33	4+209.00	Crown	5	160	0.031	1.88

3.5 Rock Burst Case Description

- **Construction method**

The drill and Blast method was used for Tunnel excavation. The drill and blast method is a cyclic technique used to excavate hard rock tunnels by drilling a pattern of blast holes in the face, charging them with explosives, and detonating to fracture the rock. A drilling jumbo is used to drill a designed pattern consisting of cut, stoping, and perimeter holes; these holes are then charged with explosives and delay detonators, stemmed, and blasted in a controlled sequence so that the cut breaks first, followed by the surrounding rock, while the perimeter holes are fired last to control overbreak and protect the final profile. After blasting, the tunnel heading is ventilated to remove fumes, and the fragmented rock (muck) is removed using loaders or LHDs and hauled out of the tunnel. Loose blocks are scaled from the roof and walls for safety, and primary support, such as rock bolts, shotcrete, and mesh, is installed before the next drilling round begins. This method

is widely used in hydropower tunnels and other hard-rock projects because it is flexible for varying geology and alignment, although it produces blasting vibrations and potential blast-damage that must be controlled in sensitive or rock-burst-prone conditions. The blasting pattern is attached in the annex. The Drill and Blasting Pattern used in the Rolwaling Project is shown in

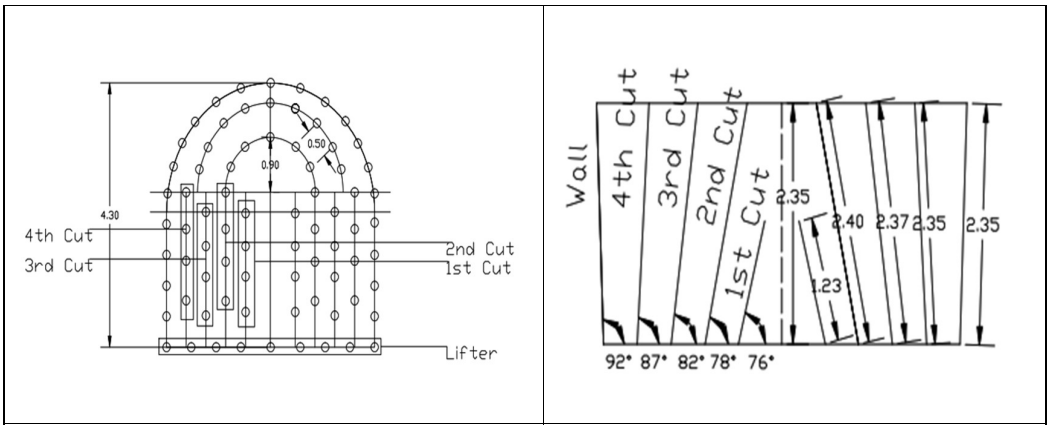

Figure 2.3: Drilling pattern in Rolwaling Khola Hydropower Project (22 MW)

- **Observed Rock burst events**

The rock mass consists of light grey colored, medium to coarse-grained, strong in strength, rough to slightly rough surface, open to tight joints, low to high persistence, thin to medium foliated Gneiss, and water condition is damp to flowing. Several rock bursts were observed with a loud cracking sound and followed by the sudden ejection of rock fragments from the wall and crown up to 2m, causing minor damage to the legs of excavators. Multiple rock cracks were observed in the Tunnel section from CH: 3+552 m to 3+742 m after 12 to 24 hrs. of blasting. In general, a rock burst occurred between 5 and 12 hours after the blast. The locations of recorded rock bursts are summarized in the table below.

Table 3.2: Rock burst details at headrace tunnel of Rolwaling Hydropower

S.N	Date	Rock Bursting Chainage	Location
1	1/1/2025	3+742.00	Left wall
2	11/1/2025	3+730.00	Right wall
3	12/1/2025	3+725.00	Left wall

4	2/2/2025	3+700.00	Left wall
5	6/2/2025	3+687.00	Left wall
6	26/3/2025	3+593.00	Right Crown
7	3/4/2025	3+580.00	Right wall
8	12/4/2025	3+565.00	Right Crown
9	12/4/2025	3+560.00	Right Crown
10	18/4/2025	3+552.00	Left wall

- **Rock burst intensity and Damage description**

Blasting at the tunnel face was temporarily suspended for periods of up to 24 hours in order to relieve stress conditions and to ensure safe working conditions for site personnel. During these stoppages, support installation was advanced in the previously excavated sections, including the installation of 3 m long rock bolts, application of shotcrete, and provision of additional spot bolts to locally strengthen the tunnel support system. Regular monitoring of the tunnel behavior was carried out throughout this period, and a 3 m long pressure-relief hole was drilled to assist in reducing stress concentration near the excavation. Safety awareness and specific instructions related to rock burst risk and stress relief measures were also communicated to the tunnel crew.

4 METHODOLOGY

4.1 Data Collection and Analysis

Data relating to rock burst incidents were carefully collected from project documents and additional sources, such as geological surveys, core logs, geological face maps, photos, and reports. These helped understand the geological and in-situ stress conditions in which the events occurred, allowing the determination of the high-risk areas along the tunnel alignment. Other data, including geological long-section and cross-section maps of the tunnel, face mapping of the excavated face, drilling and blasting patterns, the design of rock support, site inspection reports, and geology/geotechnical baseline reports, were also collected. This data provided the baseline input for numerical modelling to enable stress simulations, identification of potential rock burst zones and design of suitable support to maintain tunnel safety and integrity.

In-situ observations showed rock bursts mostly concentrated around valley zones, where stress concentrations were observed as a result of topographical effects. This phenomenon was found to be more prevalent at chainages with overburden depths of 300-380 m and lateral cover of 400-500 m. These findings are supported by previous research, which suggests that valley angles greater than 25° and maximum overburden depths of more than 500 m significantly enhance the risk of stress-induced rock mass failure, triggering underground stresses in complex topographies (Shrestha & Broch, 2008).

To assess the effect of steep valley angle on the rock burst proneness, two-dimensional models were established using finite element analysis for some chainages that represent locations of observed rock bursts. The properties of the rock mass (Geological Strength Index, deformation modulus, uniaxial compressive strength, etc.), in-situ stresses, and geometric set-ups are presented in Table 4.2 . For each chainage, two models were simulated: a non-valley model, as shown in Figure 4-2 with overburden taken from the longitudinal profile, and a valley model that took into account both longitudinal and cross-sectional profiles, as shown in Figure 4-3 and Figure 4-4 to account for stress variations due to valley slopes.

The modelling identified changes in the magnitude and direction of principal stresses, deviatoric stresses, and tangential stresses around the tunnel wall, due to the influence of topography. Higher tangential stresses in the valley model verified an increased risk of rock burst in complex topographies, informing mitigation strategies such as improved excavation methods and support design. This methodological framework is consistent with geotechnical approaches to evaluate and counter rock burst hazards for deep underground works.

4.2 Numerical Modelling and Validation

Software Used: Rocscience Phase 2

Phase2 is a two-dimensional finite element analysis software by Rocscience used to assess stress, strain and stability in rocks and soils. This program is commonly applied in underground excavation and rock mechanics projects for its capability to model complex geotechnical conditions and material properties. Phase 2 includes constitutive models like the Hoek-Brown failure criterion and Mohr-Coulomb criterion, which enable realistic modeling of rock mass behavior in terms of strength and failure under different stress regimes. Phase 2 is employed in rock burst research to model stress redistribution around underground excavations and to detect areas of stress concentration and potential failure

In rock burst studies, Phase 2 is used to analyze stress redistribution around underground openings and to identify zones of high stress concentration and potential failure. Although it does not directly simulate dynamic rock burst events, it provides important indicators such as strength factor, yielded zones, and stress distribution, which are essential for assessing rock burst susceptibility. These outputs help in understanding the mechanical response of rock masses under high in-situ stress conditions and support the design of safer excavation systems by highlighting critical areas prone to instability. Tunnel geometry and excavation parameters for numerical modelling and analysis are shown in *Table 4.1* below.

Table 4.1: Tunnel geometry and excavation parameters

Parameters	Value
Shape	Inverted D
Excavated Width	4 m
Excavated Height	4 m
Excavation Support Ratio (ESR)	1.6
Adopted Equivalent Size	2.5

In the Headrace Tunnel of Rolwaling Hydropower Project, rock bursting occurred at approximately 200 m upstream and downstream of the steep valley location as shown in the Figure below. Cracks and spalling have been observed on the tunnel walls and at the onset of the arch section. In the shotcrete areas, crack widths in the rock mass vary from a few millimeters to approximately 50 mm, accompanied by numerous hairline cracks throughout the rock. Spalled rock skin extends to depths of 20–30 cm. The primary wall crack occurs at an overburden depth of 300-380 m and lateral cover of about 500 m, corresponding to chainage in the valley region per the longitudinal profile of the HRT as shown in Figure 4.1.

The build-up of additional pressure due to valley might be the probable reason for rock bursting along this region. So, to ensure it the model was run with and without valley model and the respective output were analyzed and compared. The input parameter for model was taken from the respective face map. All the 10 rock bursting chainages were modelled and analyzed as shown in figure below. Hence, analysis was done with and without valley model to know the effect of steep valley on induced stress that might have a role in rock bursting.

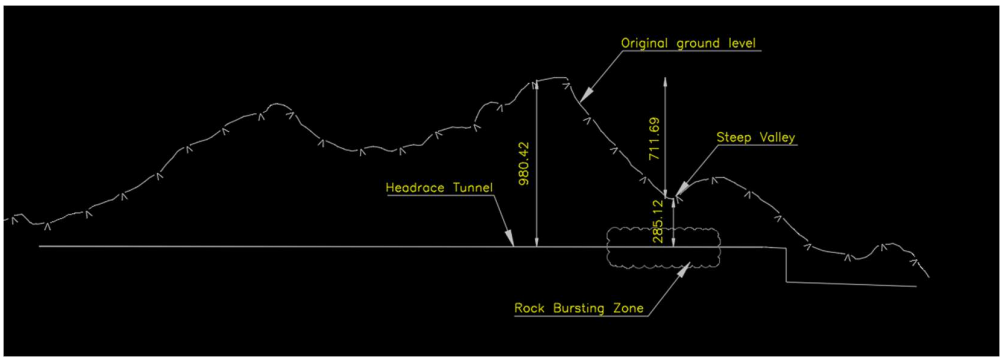

Figure 4.1: Figure showing HRT profile and rock burst region

4.2.1 Non-valley model

For the initial analysis, all rock burst chainages were modelled without creating valley geometry, and the induced stresses were obtained from the simulation results. The overburden at each chainage was simply taken from the longitudinal profile based on its respective position, whereas the lateral cover was assumed to be about 400-500 m. The parameters used for the non-valley model are presented in Table 4.2 below. Typical model for Non-Valley Model is shown in Figure 4.2.

Table 4.2: Parameters used in the non-valley model

Parameters	Remarks
Failure Criterion	Generalized Hoek and Brown
GSI	From the Respective Chainage Face map
Hoek and Brown Constant Parameters	From Rock Science Phase 2
UCS	69 Mpa (From Project Report)
Disturbance Factor	0.4
Material Type	Plastic

Young's modulus of Intact Rock	60.23 GPA (From Tamakoshi V Project)
Poisson Ratio of Intack Rock (Gneiss)	0.20
K	1.5

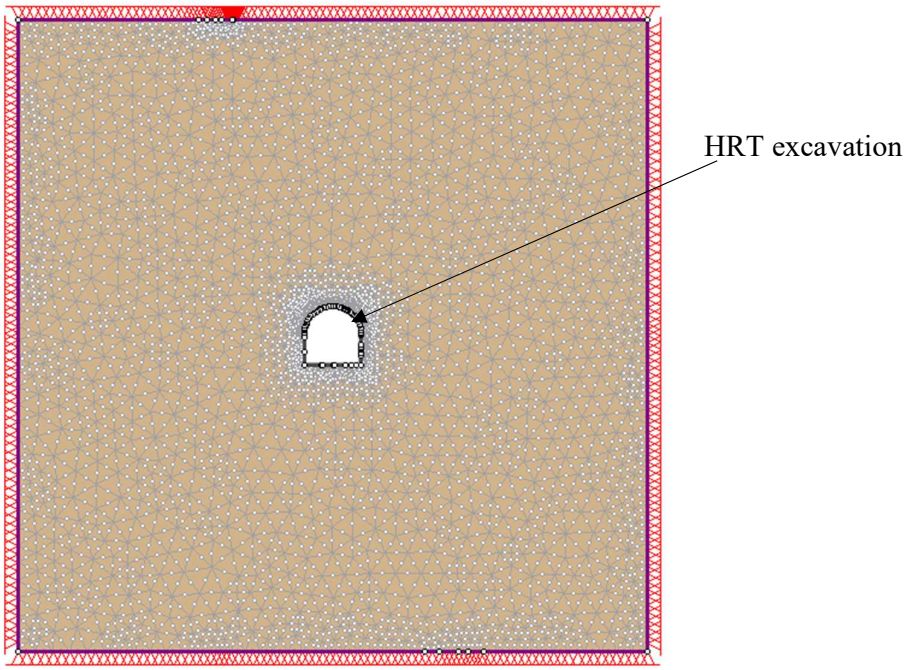

Figure 4.2: Typical non-valley model

4.2.2 Valley model

In the design of a Headrace Tunnel (HRT), modelling the valley in Rocscience Phase 2 is essential for evaluating rock burst potential, as valleys significantly influence the in-situ stress distribution. The presence of a valley reduces the overburden locally and generates stress concentrations along the slopes, causing rotations of the principal stresses. Neglecting the valley geometry can lead to an underestimation or misidentification of high-stress zones, which are most vulnerable to rock bursting. By incorporating the valley profile into the Phase2 model, the redistribution of stresses due to excavation can be accurately captured,

including tangential and radial stress components around the tunnel, critical factors for identifying areas prone to bursting.

Valley modelling also ensures the correct application of rock burst assessment criteria, such as stress ratios and strain energy density, which are highly dependent on the local stress state. Additionally, it allows for the identification of critical sections along the tunnel, including steep slope overpasses and portal regions, where support requirements may differ. Failure to model the valley might lead to inaccurate design solutions, either under designed or overdesigned. In this research, both the longitudinal and cross-sectional valley profiles were modelled to examine the effects of steep valley slopes on the in-situ induced stresses, as shown below in Figure 4.3 and Figure 4.4, respectively. To assess the contribution of topographic effects on the stress distribution and risk of rock burst, analyses were carried out at various chainages with two modelling approaches, with and without valley geometry (valley model and non-valley model, respectively). The non-valley model, in Figure 4-2, used the longitudinal profile of the surface to assign overburden pressures, assuming a flat topography. On the other hand, the valley model considered both the longitudinal and cross-sectional valley profiles, allowing for a realistic assessment of the topographic stress effects, such as valley closure and arching.

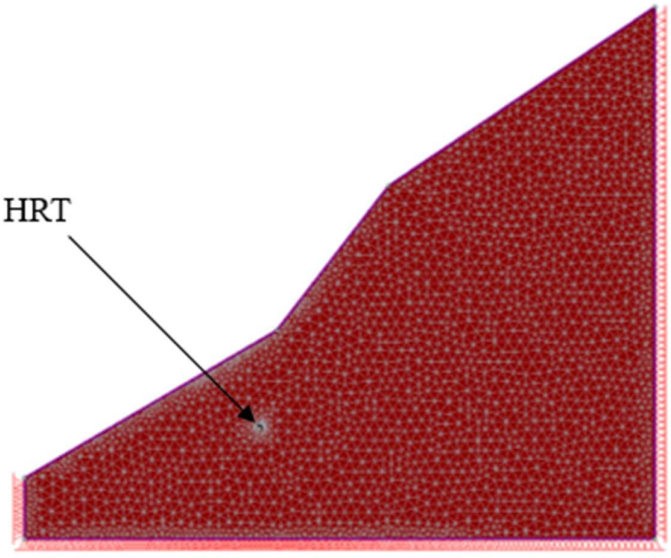

Figure 4.3: Typical CVM across HRT alignment

4.2.3 Model of preventive measures

This research evaluates the two preventive measures of rock bursts. They are stress relief holes and an optimized rock support system.

Stress Relief Holes

Drilling Pressure Relief Boreholes (DPR) are drilled after excavation in tunnel walls to prevent rock bursts by relieving high tangential stress and elastic strain energy. These holes create local deformation and fractures, establishing a plastic damage zone which relocates the high stress away from the excavation surface and forms a low-stress buffer zone surrounding the excavation, resulting in the reduction of micro seismic events, weakening strain build-up, and redistribution of stress concentrations. Optimal performance relies on parameters like borehole diameter, length, spacing, and density. Larger diameters and denser arrays can achieve 12-33% stress reduction and lower acoustic emission events, often complementing destress blasting or dynamic supports in high-stress deep tunnelling and mining applications where they preempt violent ejections and downgrade burst severity from strong to moderate.

To evaluate the impact of stress relief holes, four holes (Diameter 30 cm and spacing 1.5 m) were modelled and analyzed. Two initial scenarios were considered: one with holes at the center of the face and another with holes at the excavation periphery, as shown in Figure 4.4 and Figure 4.5, respectively. These features 30 cm diameter holes spaced 1.5 m apart. However, implementing 30 cm diameter holes may not be practical at the site, prompting evaluation of smaller 15 cm diameter holes spaced 75 cm apart at the top crown periphery above the spring line, as shown in Figure 4.6. A comparative analysis assessed the effectiveness of the 30 cm holes (1.5 m spacing) versus the 15 cm holes (75 cm spacing).

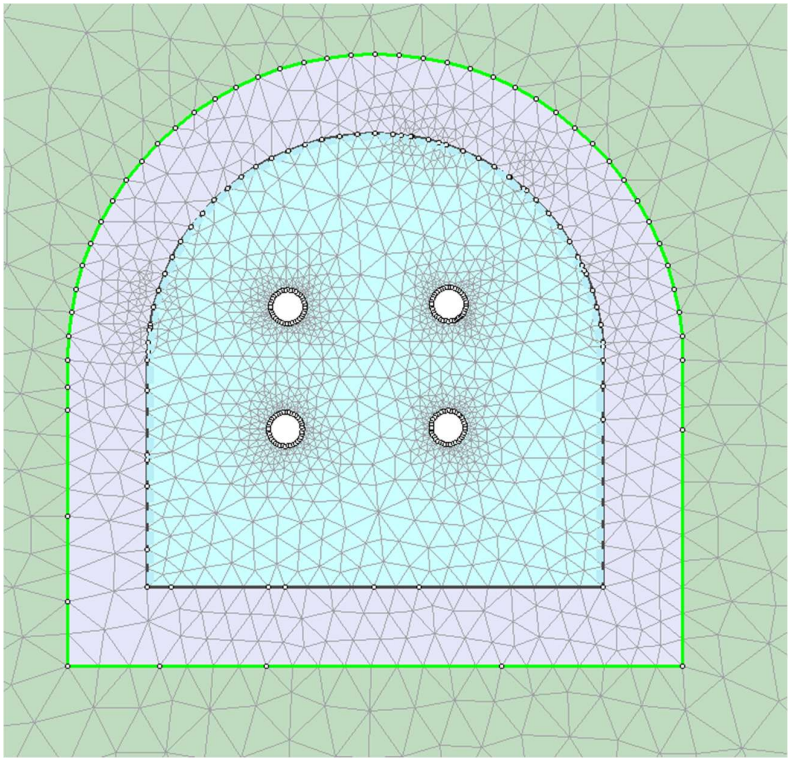

Figure 4.4: SRH of 30 cm dia at 1.5 m spacing at the center of the face

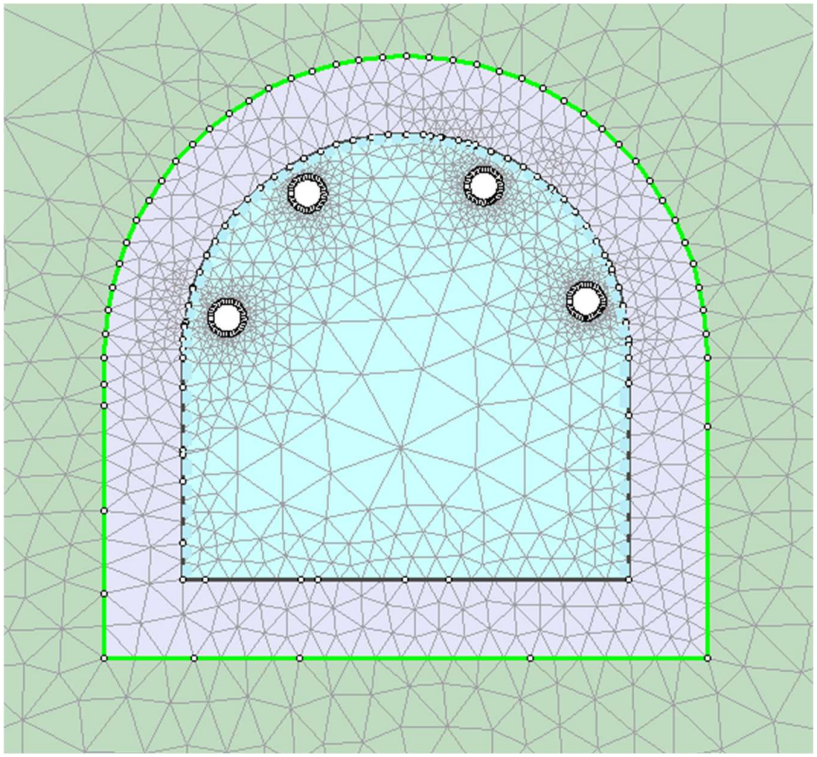

Figure 4.5: SRH of 30 cm dia at 1.5 m spacing at excavation periphery

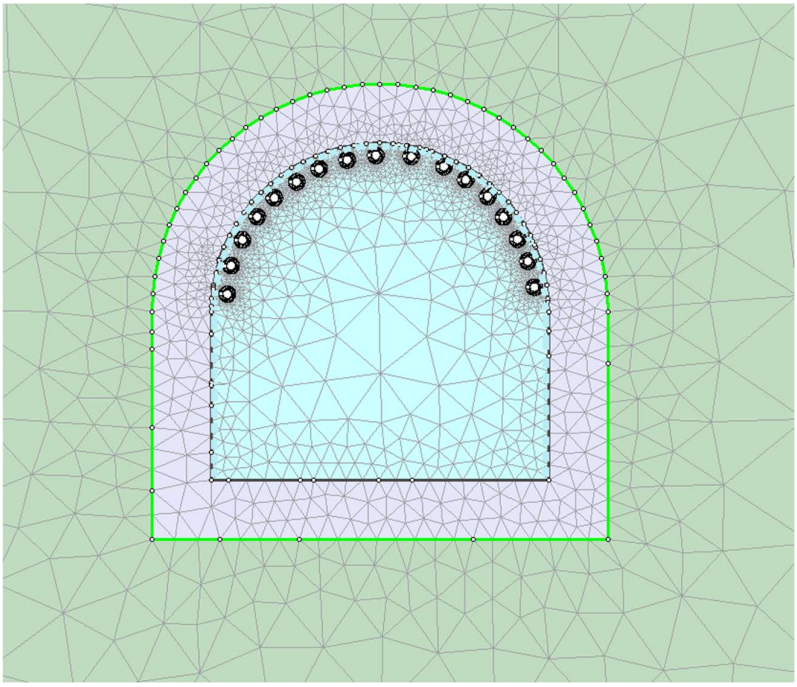

Figure 4.6: SRH of 15 cm dia at 50 cm spacing at excavation periphery

Rock Support System

Rock support systems like shotcrete and lockbolts are essential for preventing rock bursts in deep tunnels or mines, where intense underground pressures can cause rock to suddenly fracture and violently eject debris. Shotcrete, a type of concrete that can be sprayed onto a surface, often with reinforcing steel fibers or wire mesh, is sprayed onto the surface of the newly excavated wall to create a skin-like membrane that catches small spalls, redistributes loads, and prevents minor falls from becoming bigger problems, often in 50-150 mm thick layers. Rock bolts, long steel bars anchored into stable rock deep into the tunnel wall, are like stitches to bind the separated layers together; in areas prone to bursting, energy-absorbing or "yieldable" rock bolts deform or slip in the face of explosive forces, cushioning the impact and permitting limited deformation. Together, rock bolts support from behind and shotcrete coats the face right after excavation (with faceplates and mesh for additional strength) to convert potentially fatal snaps into safe, controlled movements like a seatbelt and an airbag that protect your life, without the concrete being too rigid. At Chainage 3+530, the rock burst incident damaged the rock bolt and Shotcrete, as shown in Figure 4.7 below:

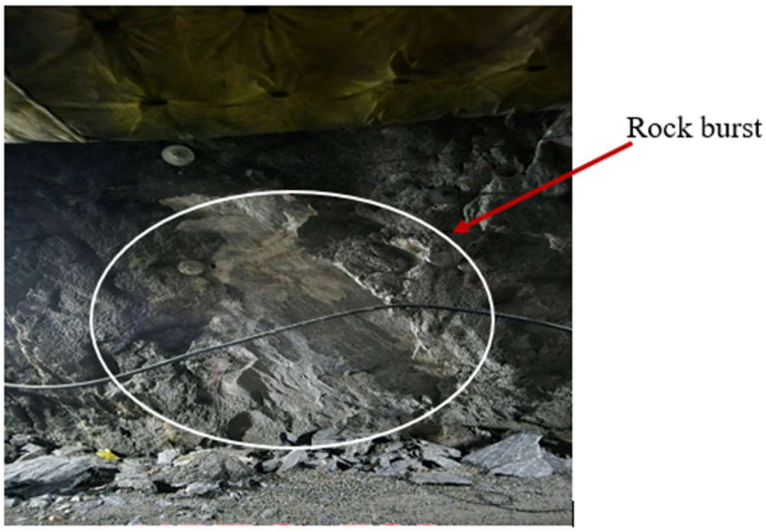

Figure 4.7: Rock bolt and shotcrete failure at Ch. 3+530 m due to rock burst

The same rock bolt and shotcrete systems were modelled and analyzed using RocScience Phase 2. Properties for the shotcrete and rockbolts were taken from the project's rock support drawings and are listed in Table 4.3 and Table 4.4 respectively. Subsequently, these properties were modified, and the systems were re-modelled and re-analyzed as shown in Figure 4.9, with the updated parameters presented in the respective Table 4.5 and Table 4.6.

Table 4.3: Properties of shotcrete at Ch. 3+530 m as per rock support drawing

Shotcrete properties	**Values**	**Reference**
Characteristic Compressive Strength (MPa)	30	
Young's modulus, E (MPa)	27,386	$5000\sqrt{fck}$ (IS: 456)
Mean Tensile Strength (MPa)	3.83	$0.7\sqrt{fck}$ (IS: 456)
Thickness (cm)	10	As per the rock support

Table 4.4: Rock bolts properties at Ch. 3+530 m as per rock support drawing

Grouted bars properties (fully cement grouted)	**Values**	**Grouted bars properties (fully cement grouted)**	**Values**
Diameter of grouted bars (mm)	25	Spacing of rock bolt(m)	2
Tensile Capacity (MN)	0.15	F_y(Mpa)	450
Effective Area of Steel (mm^2)	415.48		
Length of Rock Bolt(m)	2.5		

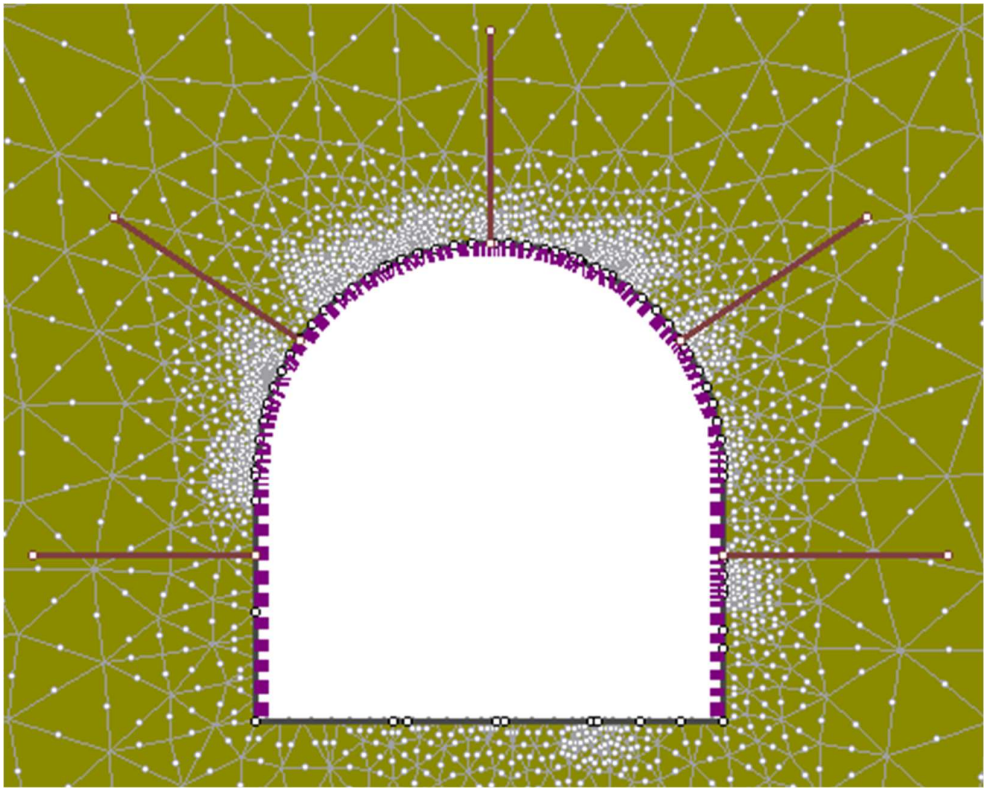

Figure 4.8: Rock support system at Ch. 3+530 m as per support drawings

Table 4.5: Modified properties of shotcrete at Ch. 3+530 m

Shotcrete properties	**Values**	**Reference**
Characteristic Compressive Strength (MPa)	30	
Young's modulus, E (MPa)	27,386	$5000\sqrt{fck}$ (IS: 456)
Mean Tensile Strength (MPa)	3.83	$0.7\sqrt{fck}$ (IS: 456)
Thickness (cm)	15	As per the rock support drawings
Wire mesh dia (mm)	6	

Table 4.6: Modified properties of rock bolt at Ch. 3+530 m

Grouted bars properties (fully cement grouted)	**Values**	**Grouted bars properties (fully cement grouted)**	**Values**
Diameter of grouted bars (mm)	25	Spacing of rock bolt(m)	1.5
Tensile Capacity (MN)	0.15	F_y(MPa)	450
Effective Area of Steel (mm^2)	415.48		
Length of Rock Bolt(m)	2.7		

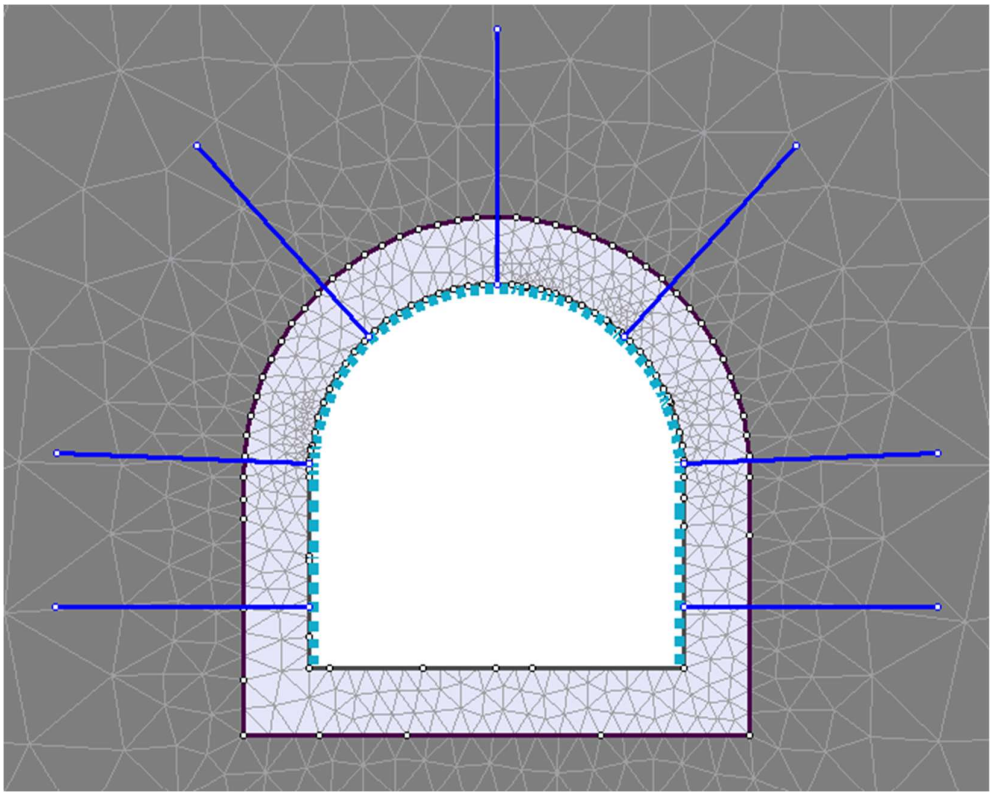

Figure 4.9: Model of modified rock support system at Ch. 3+530 m

The different stages that have been implemented in the modelling are described below:

Stage 1: This stage is the development of the initial in-situ stress condition before any excavation. In Rocscience Phase2, the model is regarded as a continuous and undisturbed rock mass in which field conditions are simulated by applying gravitational loading and predefined stress ratios. In most cases, vertical stress is determined with the help of overburden weight, and the horizontal stress is determined with the help of the proper lateral stress coefficient. The model is then made to reach equilibrium at this stage, and the stresses are distributed without any artificial disturbances. There is no excavation or deformation in this stage, but it is the base level by which all future stress redistribution will be gauged. In-situ stresses should be defined accurately as it plays a major role in determining the extent and distribution of the stress concentration that occurs in the course of excavation, especially in deep tunnels or high topography areas..

Stage 2: The second step is partial stress reduction in the elements that are to be excavated, which is usually carried out with the help of a stress reduction factor

(e.g., 50%). This phase is not a real removal of material but is an imitation of the progressive offloading of stresses that takes place before the progressive face of the tunnel. This is because the analysis takes place in two dimensions, and hence the approach estimates the three-dimensional effects relating to tunnel progress. The model predicts a steady redistribution of stresses and the onset of localized yielding about the future tunnel boundary by reducing the internal stresses in the excavation zone. This step in the middle is to avoid unrealistic instantaneous stress release and allow a more realistic model of the mechanical response of the rock mass, particularly in brittle formations where unloading can cause large stress concentrations, and failure can be initiated.

Stage 3: The third stage is associated with the complete excavation of the tunnel, the components in the excavation boundary are deactivated or given the null material properties. The effect of this is total stress discharge in the excavated area and causes considerable redistribution of stress in the surrounding rock mass. This consequently causes the tangential stresses to grow in the boundary of the excavation and in most instances, plastic zones and localized failures are formed depending on the strength and stiffness of the rock mass. The step is important in assessing the stability of the tunnel since it indicates the largest perturbation of the pre-existing stress field. In stressful geological conditions, like in deep tunnels or steep slope valley conditions, this phase can also denote areas where rock burst could occur because of the accumulated elastic strain and the sudden change in stresses.

Stage 4: The fourth stage means the support elements are installed to model the interaction between the excavated rock mass and the reinforcement system. Rock bolts, shotcrete lining or steel sets are support components that are predefined in Rocscience Phase2 but triggered once excavation has been made to represent realistic construction activity. The delayed activation permits the pre-load initial deformation and redistribution of stress to happen before the commencement of the support carrying the load, which is similar to field methods such as the New Austrian Tunnelling Method. Upon installation, the support system will act in collaboration with the surrounding rock mass and distribute the load, which will increase the confinement and minimize further deformation. The rigidity, strength and timeliness of the support used determine its success in removing stress and stabilizing the structure, and these factors affect the degree of redistribution of stress and structural stability.

5 RESULTS AND DISCUSSION

The results from numerical analysis in RS2 (Rocscience Phase 2) have been categorized into two sections.

5.1 Non-Valley and Valley Effect

After numerical modelling and analysis of all the rock burst chainages, the induced stresses were estimated for the different model (Valley Model and Non-Valley Model) types. The results are presented in the following figure and tables.

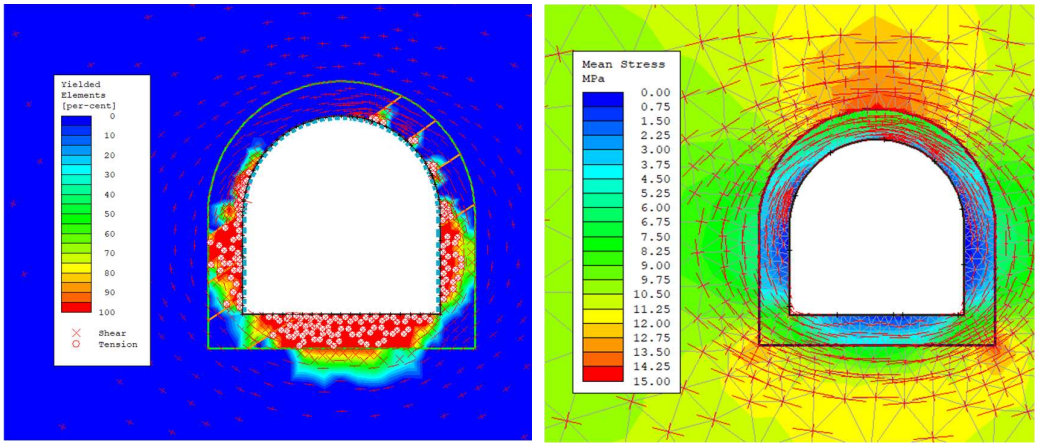

Figure 5.1: Result of the non-valley model of Ch. 3+552 m and 3+560 m

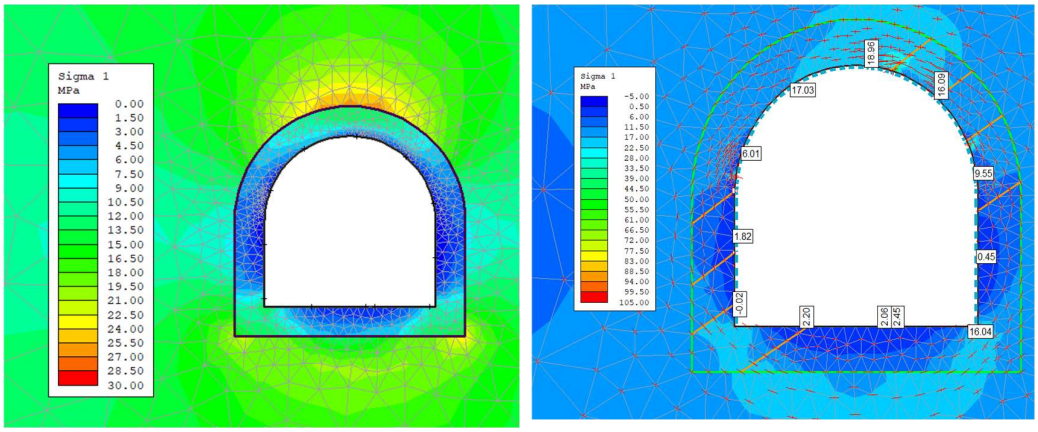

Figure 5.2: Result of the non-valley model of Ch. 3+565 m and 3+580 m

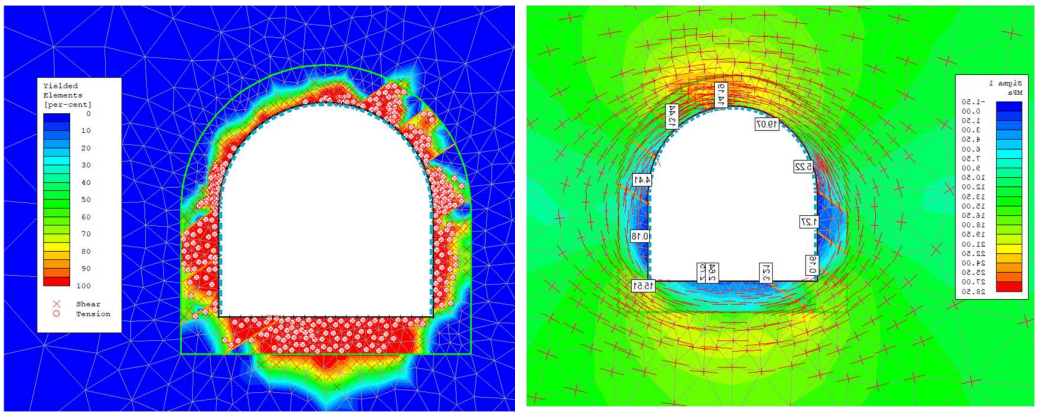

Figure 5.3: Result of the non-valley model of Ch.3+593 m and 3+687 m

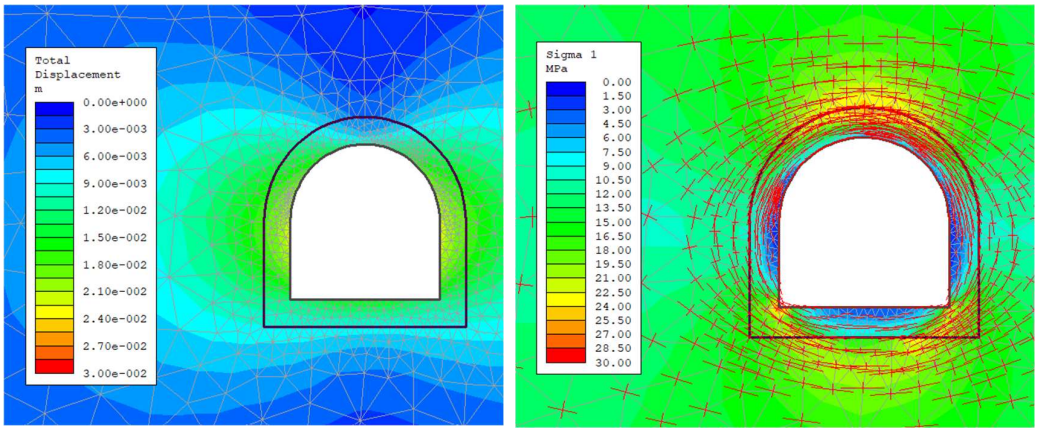

Figure 5.4: Result of the non-valley model of Ch. 3+700 m and 3+725 m

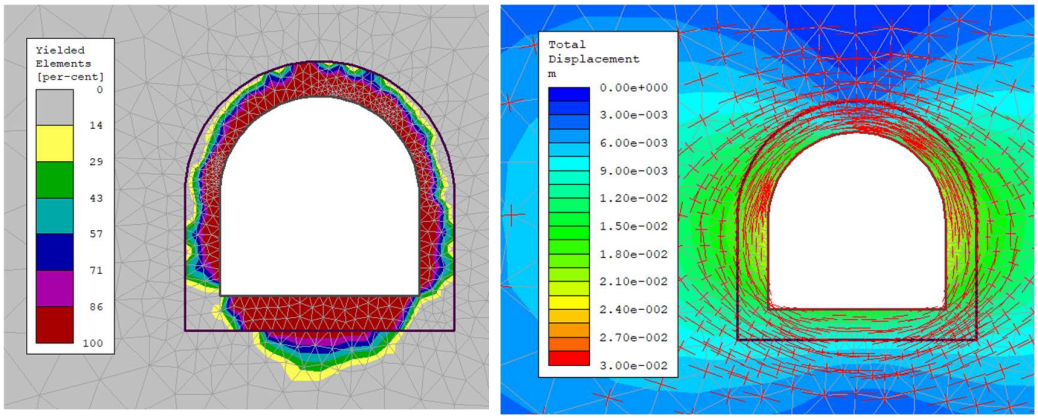

Figure 5.5: Result of the non-valley model of Ch. 3+730 m and 3+742 m

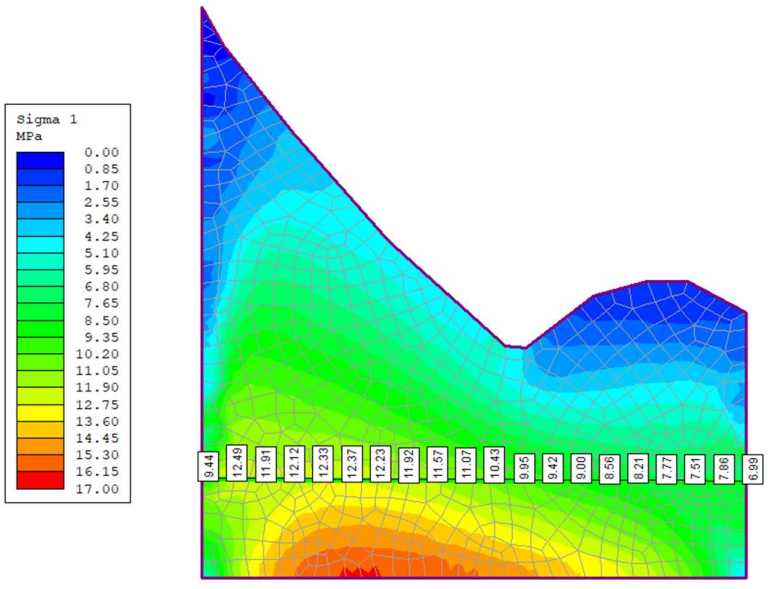

Figure 5.6: Principal major in situ stress at different chainages from the LVM

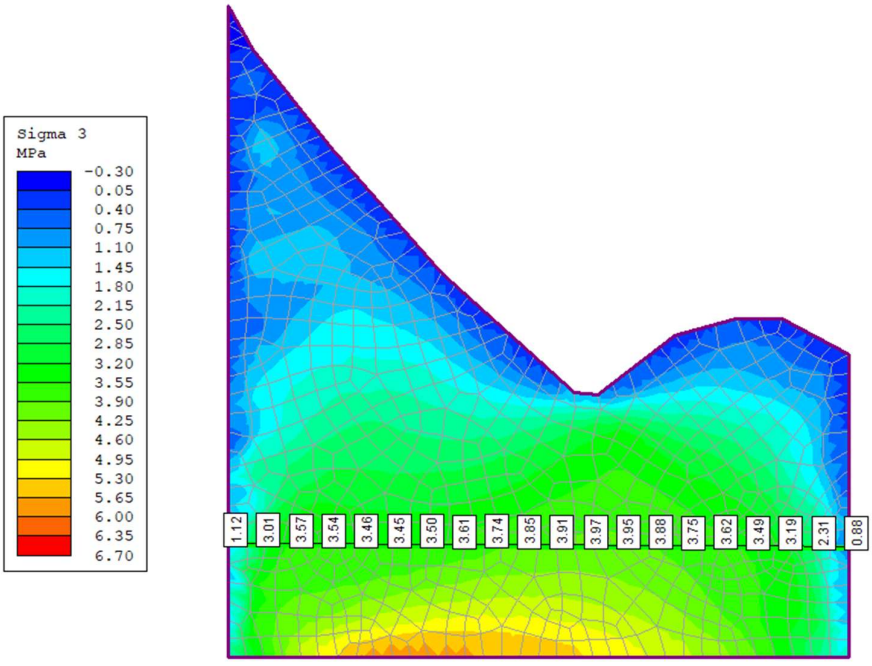

Figure 5.7: Principal minor in situ stress at different chainages from the LVM

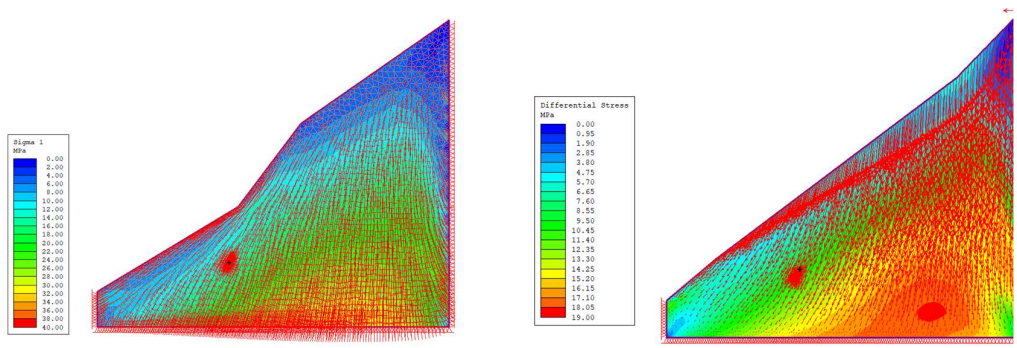

Figure 5.8: Result from CV Model at Ch. 3+552 m and 3+560 m

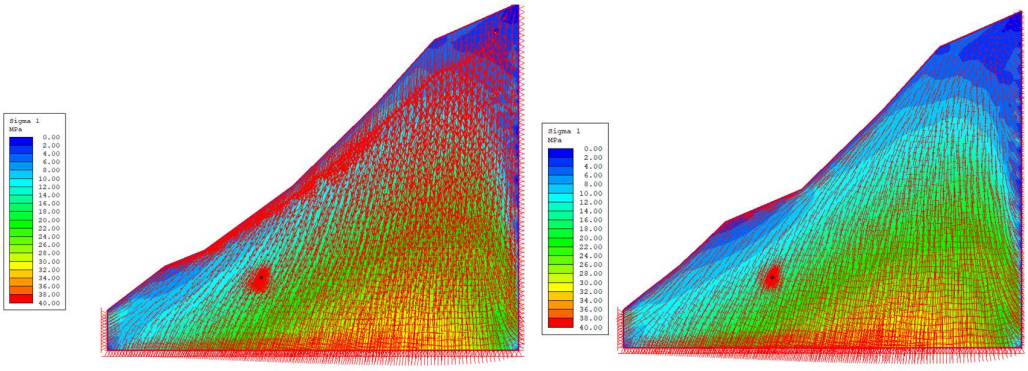

Figure 5.9: Result from CV Model at Ch. 3+565 m and 3+580 m

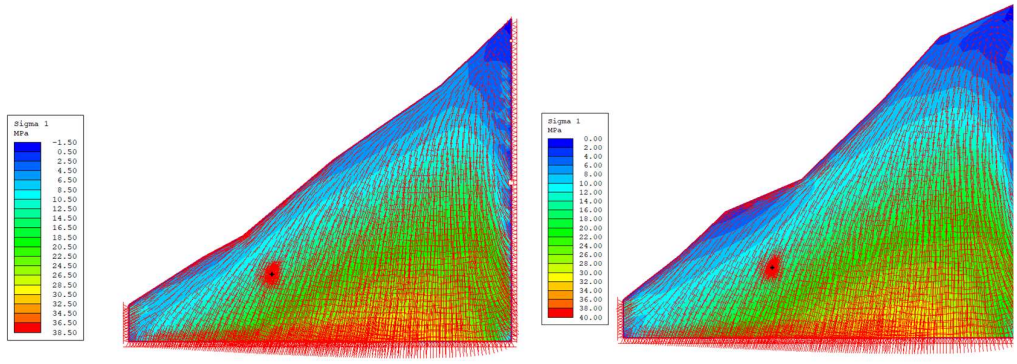

Figure 5.10: Result from CV Model at Ch. 3+593 m and 3+687 m

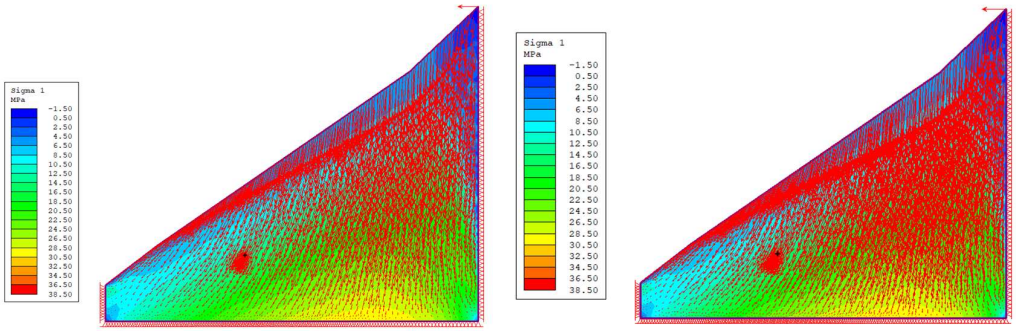

Figure 5.10: Result from CV Model at Ch. 3+700 m and 3+725 m

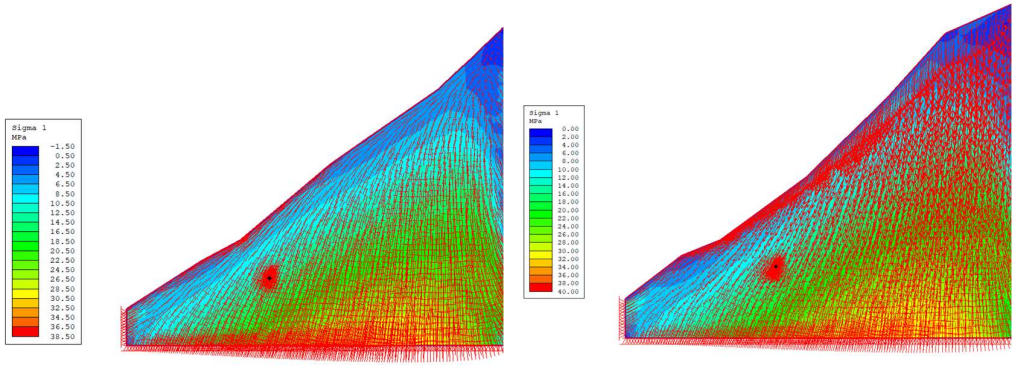

Figure 5.11: Result from CV Model at Ch. 3+730 m and 3+742 m

Table 5.1: Different induced stresses obtained from the non-valley model

Rock burst Chainages	Principle Major Stress $(\sigma_1)'_{max}$	Principle Minor Stress $(\sigma_3)'_{max}$	Tangential stress $(\sigma_\theta)'_{max}$	Deviatoric Stress $(\sigma_1'-\sigma_3')$	σ_θ/σ_c
	Mpa	Mpa	Mpa	Mpa	
3+552	17.36	6.12	45.96	11.24	0.67
3+560	18.96	5.94	50.94	13.02	0.74
3+565	18.46	4.11	51.27	14.35	0.74
3+580	18.96	5.94	50.94	13.02	0.74

Rock burst Chainages	Principle Major Stress $(\sigma_1)'_{max}$	Principle Minor Stress $(\sigma_3)'_{max}$	Tangential stress $(\sigma_\theta)'_{max}$	Deviatoric Stress $(\sigma_1'-\sigma_3')$	σ_θ/σ_c
	Mpa	Mpa	Mpa	Mpa	
3+593	17.23	4.22	47.47	13.01	0.69
3+600	18.22	5.43	49.23	12.79	0.71
3+687	18.55	5.11	50.54	13.44	0.73
3+700	17.65	5.83	47.12	11.82	0.68
3+730	17.8	4.86	48.54	12.94	0.70
3+742	18.24	4.21	50.51	14.03	0.73

Table 5.2: Different induced stresses obtained from LVM

Rock burst Chainages	Principle Major Stress $(\sigma_1)'_{max}$	Principle Minor Stress $(\sigma_3)'_{max}$	Tangential stress $(\sigma_\theta)_{max}$	Deviatoric Stress $(\sigma_1'-\sigma_3')$	σ_θ/σ_c
	Mpa	Mpa	Mpa	Mpa	
3+552	22.11	3.16	63.17	18.95	0.92
3+560	21.22	3.43	60.23	17.79	0.87
3+565	21.11	3.43	59.9	17.68	0.87
3+580	21.98	3.43	62.51	18.55	0.91

Rock burst Chainages	Principle Major Stress $(\sigma_1)'_{max}$	Principle Minor Stress $(\sigma_3)'_{max}$	Tangential stress $(\sigma_\theta)_{max}$	Deviatoric Stress $(\sigma_1'-\sigma_3')$	σ_θ/σ_c
	Mpa	Mpa	Mpa	Mpa	
3+593	20.36	4.12	56.96	16.24	0.83
3+600	21.04	3.96	59.16	17.08	0.86
3+687	22.11	4.8	61.53	17.31	0.89
3+700	22.35	3.84	63.21	18.51	0.92
3+730	17.8	4.86	48.54	12.94	0.70
3+742	18.24	4.21	50.51	14.03	0.73

Table 5.3: Different induced stresses obtained from the CVM

Rock burst Chainages	Principle Major Stress $(\sigma_1)'_{max}$	Principle Minor Stress $(\sigma_3)'_{max}$	Tangential stress $(\sigma_\theta)_{max}$	Deviatoric Stress $(\sigma_1'-\sigma_3')$	σ_θ/σ_c
	Mpa	Mpa	Mpa	Mpa	
3+552	23.98	3.26	68.68	20.72	0.99
3+560	23.21	4.2	65.43	19.01	0.95
3+565	23.21	4.2	65.43	19.01	0.95
3+580	23.16	3.96	65.52	19.2	0.95

3+593	23.4	4.13	66.07	19.27	0.96
3+600	22.63	3.86	64.03	18.77	0.93
3+687	23.87	4.01	67.6	19.86	0.98
3+700	23.14	3.81	65.61	19.33	0.95
3+730	22.68	4.06	63.98	18.62	0.93
3+742	24.06	4.12	68.06	19.94	0.99

The different types of induced stresses from the different types of models are also shown in the following Figure 5.12, Figure 5.13 and Figure 5-14.

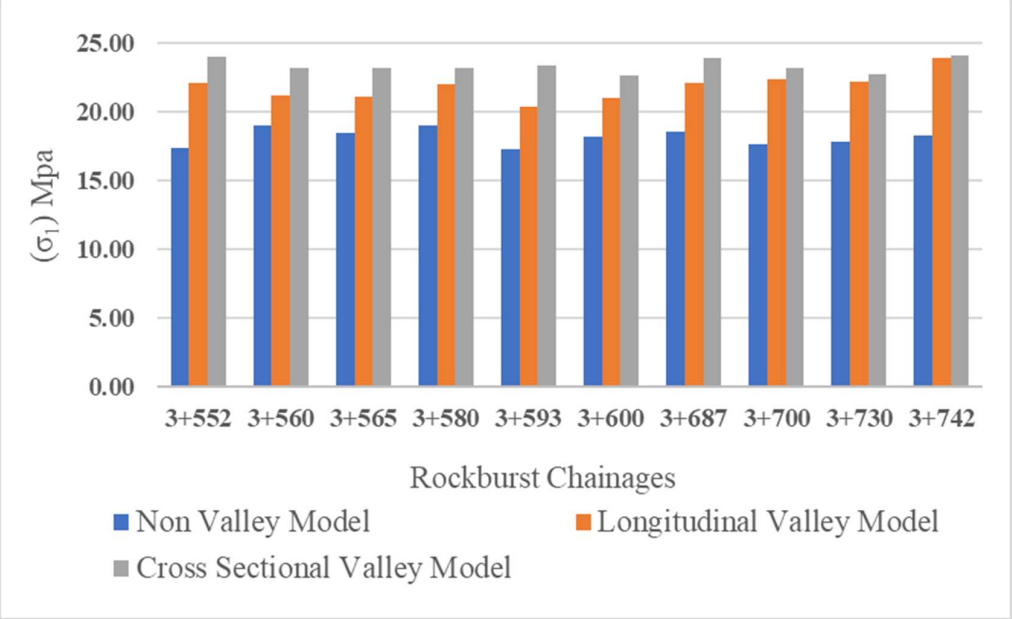

Figure 5.12: Principle major induced stress for different Models

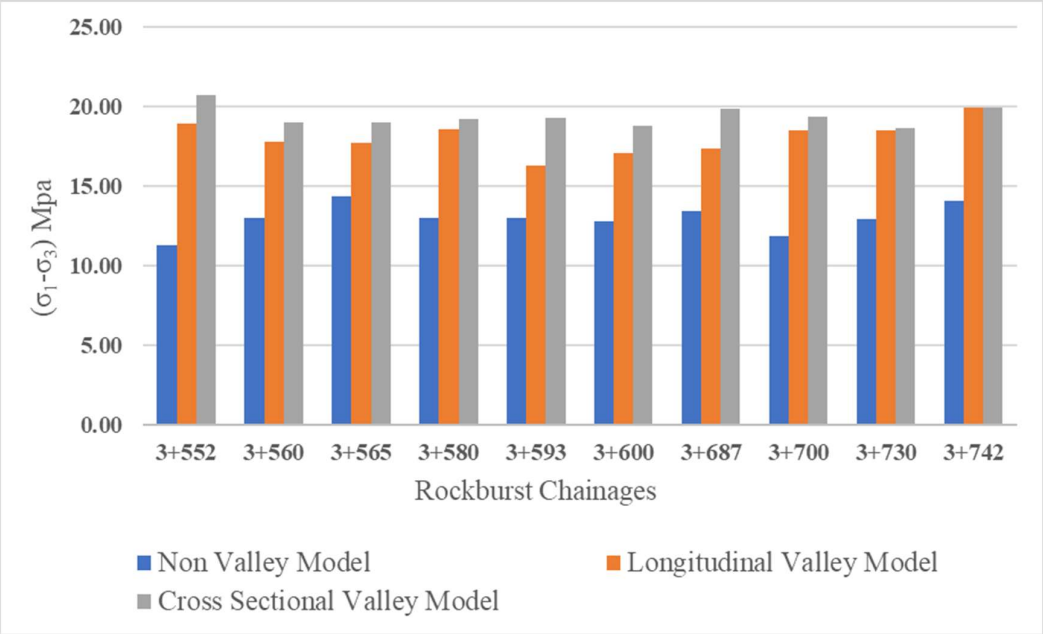

Figure 5.13: Induced deviatoric stress for different models

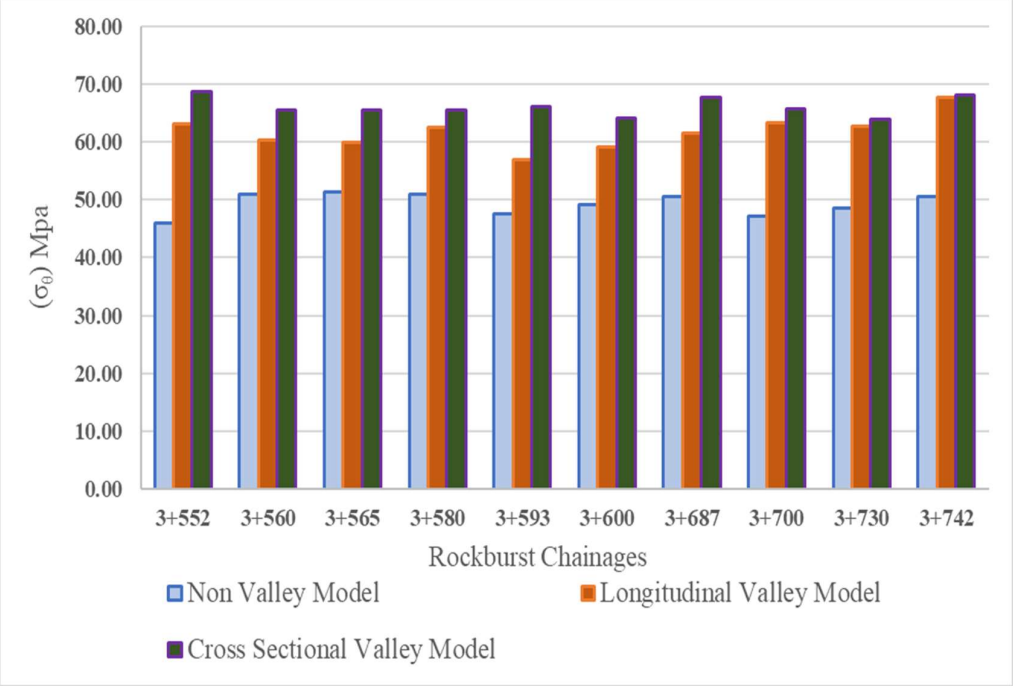

Figure 5-14: Induced tangential stress for different models

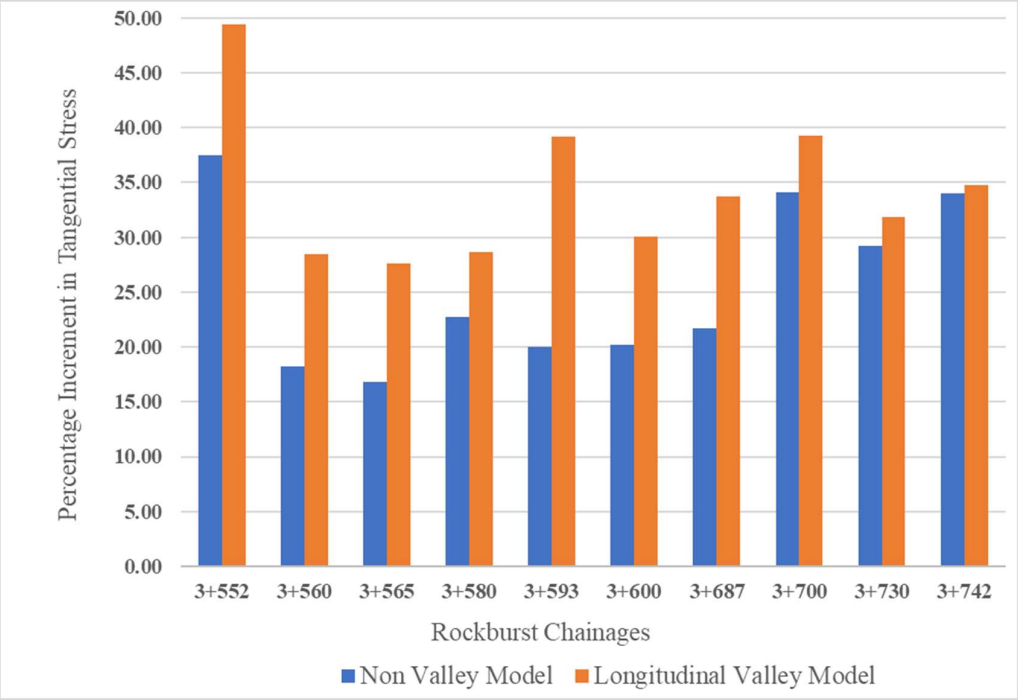

Figure 5.15: Percentage increment in tangential stress in the valley model

5.2 Preventive Measures

This section presents the outcomes of numerical modelling for rock burst preventive measures. It covers two aspects: (1) stress relief holes with varying diameters and spacings around the tunnel, and (2) the rock support system design outlined in the Methodology section.

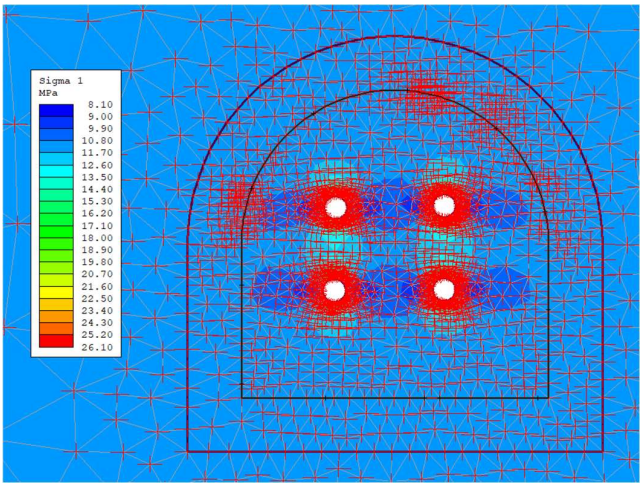

Figure 5.16: Result of 30 cm diameter SRH at 1.5 m spacing (At Centre)

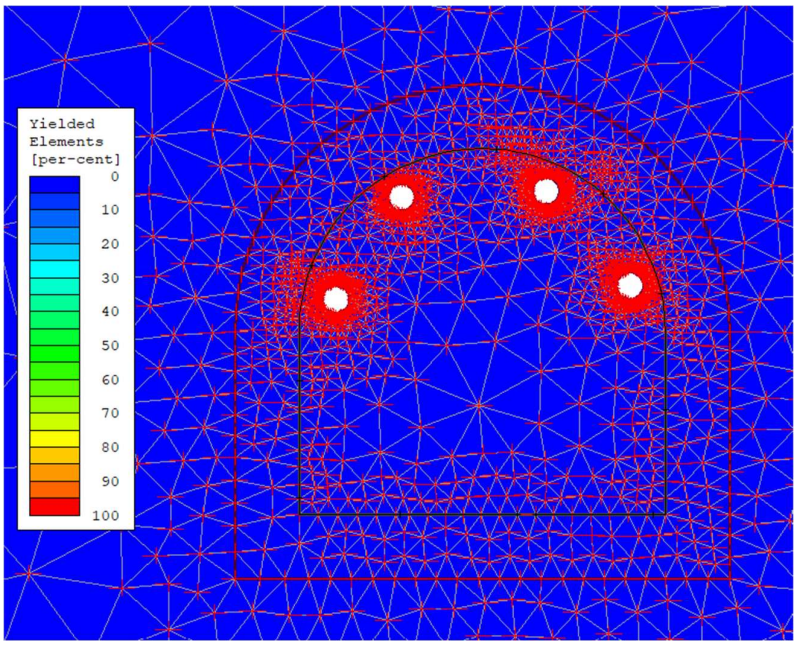

Figure 5.17: Result of 30 cm diameter SRH at 1.5 m spacing (At Periphery)

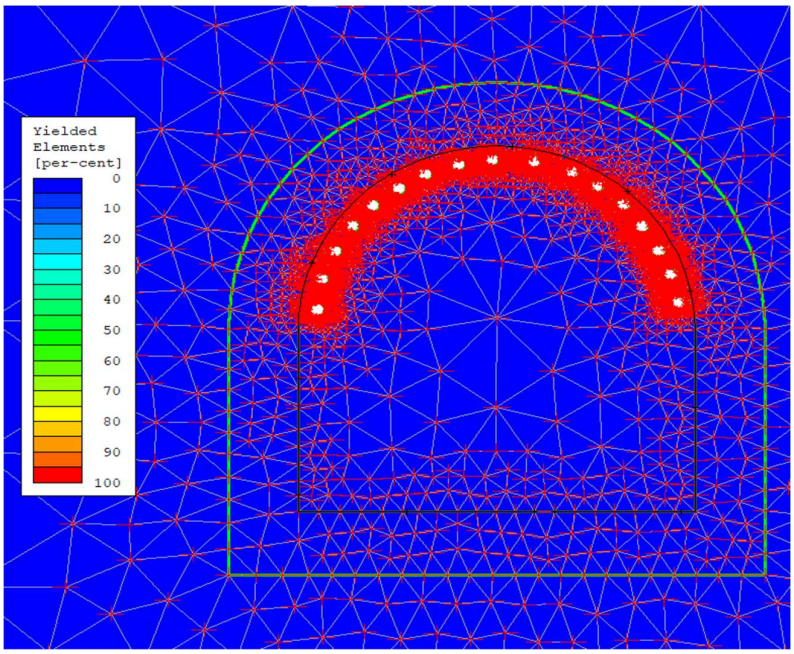

Figure 5.18: Result of 15 cm diameter SRH at 0.5 m spacing (At Periphery)

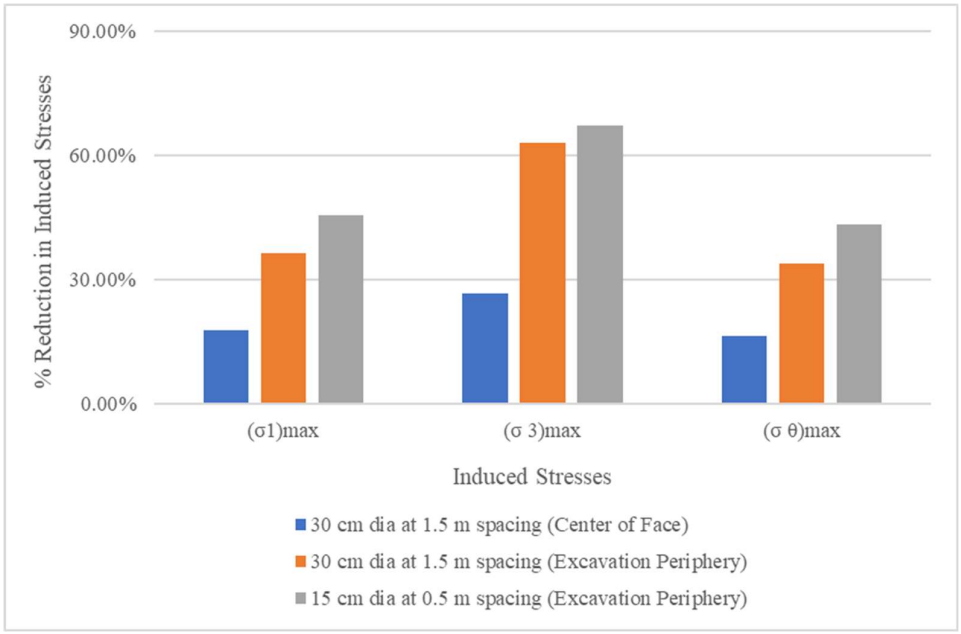

Figure 5.19: Reduction in induced stresses for different SRH

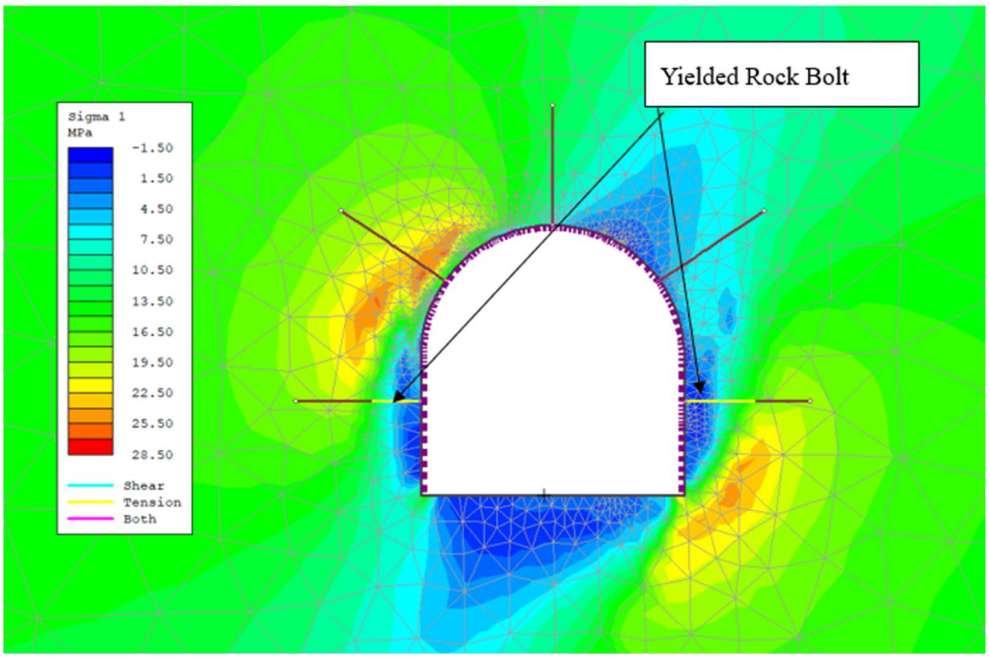

Figure 5.20: Result of rock support system as per actual site condition

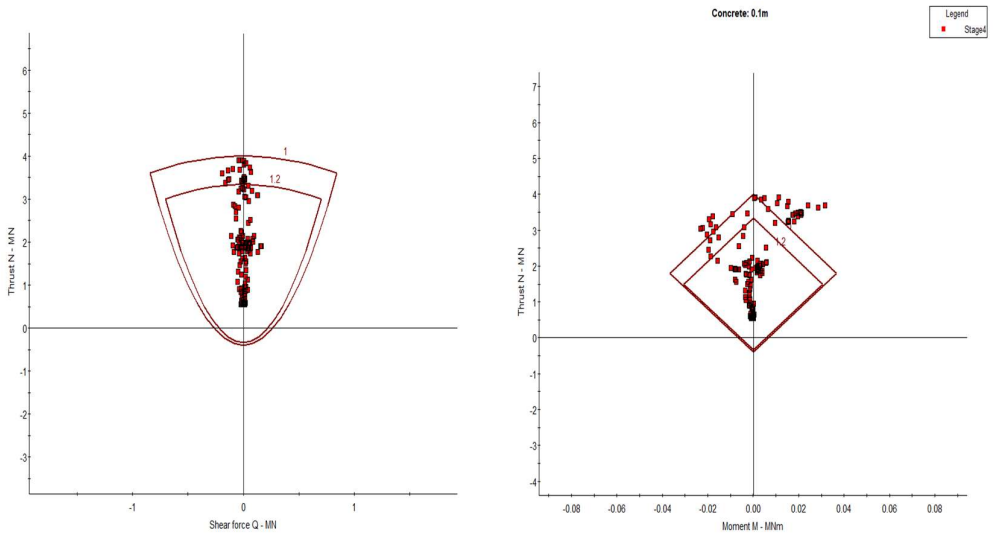

Figure 5.21: FoS showing failure of the applied shotcrete at Ch. 5+530

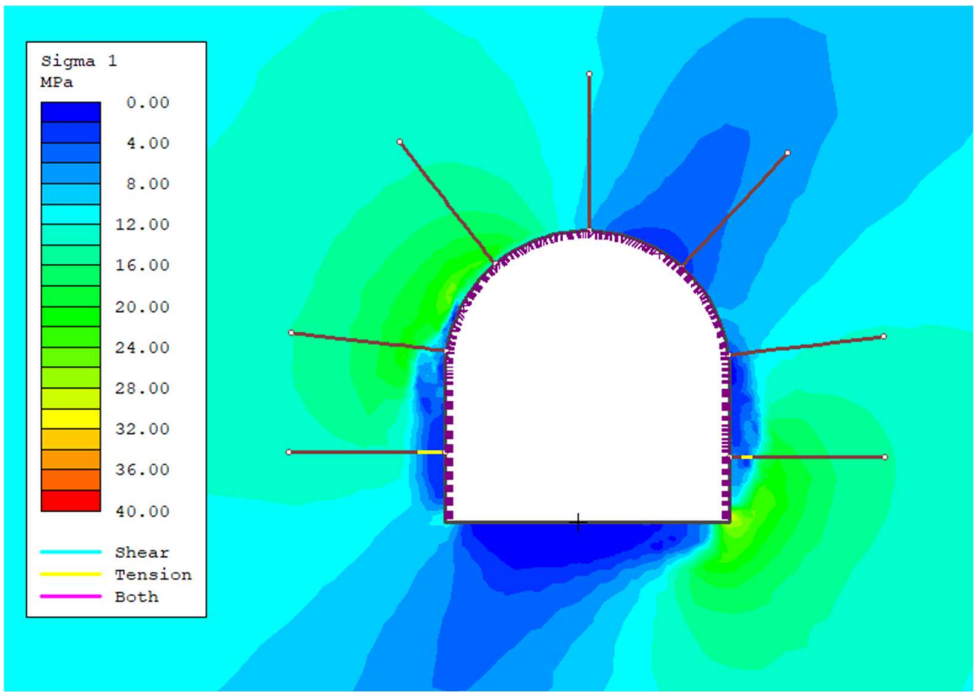

Figure 5.22: Result of the modified rock support system

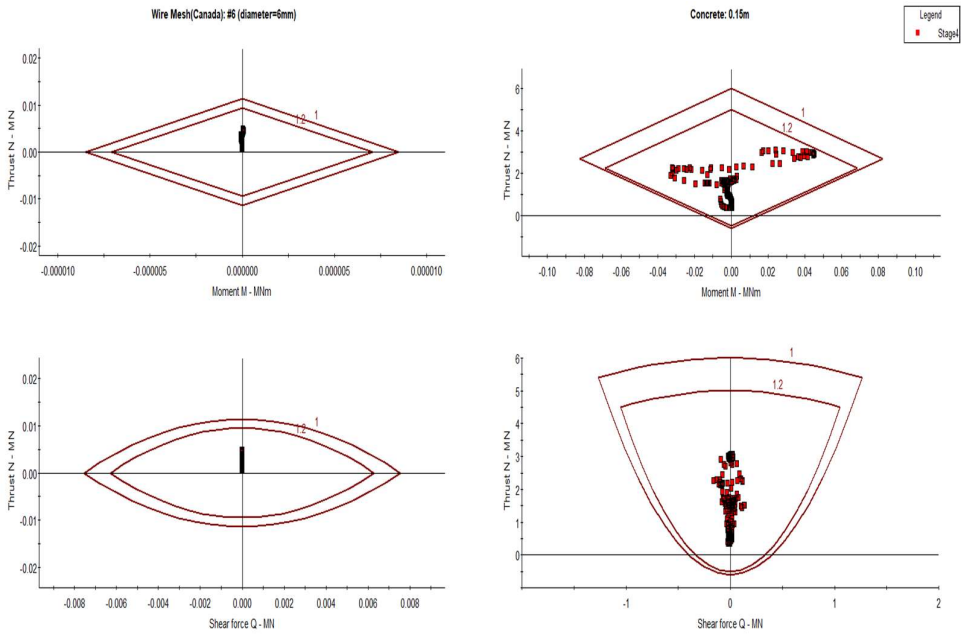

Figure 5.23: FoS of stable condition of the modified shotcrete at Ch. 5+530

The numerical analysis demonstrates that valley geometry has a significant influence on the induced stress distribution along the tunnel alignment. In the absence of valley effects, the major principal stresses (σ_1, σ_3) and tangential stress (σ_θ) remain within moderate limits, indicating a relatively stable stress regime around the excavation. However, when longitudinal valley topography is introduced, stress magnitudes increase due to variations in overburden pressure along the tunnel axis. This effect becomes more pronounced under cross-sectional valley conditions, where the highest tangential stresses (approximately 63–66 MPa) are observed. The stress ratio (σ_θ/σ_c) approaching unity (0.93–0.99) suggests that the induced stresses are nearly equal to the rock mass strength, indicating a critical condition prone to rock burst failure.

The variation of tangential stress across different chainages further highlights the dominant role of valley geometry. The non-valley model consistently produces the lowest stress values, while the longitudinal valley model shows moderate stress amplification. In contrast, the cross-sectional valley condition generates the highest stress concentrations at all chainages, confirming that transverse valley effects are more critical than longitudinal variations. The increase in tangential stress due to steep valley geometry ranges from approximately 30% to 40%, with

peak amplification occurring near chainages 3+593 and 3+700. Even the minimum increase remains substantial, emphasizing that steep topography significantly intensifies in-situ stress conditions and increases the likelihood of instability and rock burst.

The analysis of stress relief holes at chainage 3+700 demonstrates the importance of both placement and spacing in mitigating stress concentration. Without any stress relief measures, the excavation experiences a critical stress state. The introduction of four holes with 30 cm diameter at 1.5 m spacing near the excavation periphery results in considerable stress reduction (36.48% in σ_1, 62.90% in σ_3, and 33.83% in σ_θ), indicating that peripheral placement effectively targets zones of maximum stress concentration. Further improvement is achieved with smaller diameter holes (15 cm) at closer spacing (0.50 m), which yield higher stress reductions (45.63%, 67.23%, and 43.26%, respectively). This suggests that a denser pattern of smaller holes enhances uniform stress redistribution and reduces localized stress accumulation, thereby lowering rock burst potential.

The support system evaluation at chainage 3+530 further reinforces the importance of incorporating valley-induced stresses in design considerations. The original support system, consisting of 10 cm shotcrete and 2.5 m long rock bolts spaced at 2 m, was found to be inadequate under rock burst conditions. Numerical analysis and field observations indicate tensile failure in shotcrete and yielding of rock bolts near the tunnel walls, suggesting insufficient confinement. The revised support system, comprising 15 cm shotcrete, 2.7 m long bolts, and reduced spacing of 1.5 m, shows significantly improved performance. The enhanced behavior is attributed to increased shotcrete stiffness and improved anchorage provided by longer bolts extending beyond the yielded zone into competent rock mass.

6 CONCLUSIONS AND RECOMMENDATIONS

6.1 Conclusions

The steep valley topography strongly influences stress amplification around underground excavations, and the cross-sectional geometry of the valley produces the most severe stress concentrations, thereby playing a dominant role in rock burst triggering. The findings have clearly shown that underestimating induced stresses using valley effects as a neglected factor may also result in unsafe design of tunnels. Moreover, the stress-relieving holes are highly dependent on shape; holes placed near the excavation periphery are more effective at relieving concentrated stresses, whereas smaller-diameter holes placed farther apart are more efficient at relieving concentrated stresses through more uniform redistribution.

The study also reveals that even the traditional support systems may not be effective enough with the increased stress levels which are accumulated with steep topography. The introduction of improvements to ensure that the tunnel gives a greater degree of confinement and anchorage of the tunnel has enhanced the stability of the tunnel significantly. Thus, the design approach that considers the stress effects caused by the valley, the optimization of the stress relief methods and the enhancement of the support systems are crucial to the reduction of the rock burst hazards and the safety and stability of the tunnels in the mountainous regions.

6.2 Recommendations

Due to time limitations and computational constraints, this research has several limitations which can be addressed in future. The following are some recommendations for upcoming work:

- The study assumes isotropic rock mass properties, which may influence results to some degree; incorporating rock mass anisotropy could enhance accuracy.
- This analysis uses 2D finite element modelling; future work could employ 3D finite element models for greater precision.

- Valleys were developed as two separate configurations (longitudinal and cross-sectional); advanced 3D software could integrate them into a combined model to better represent actual site conditions.
- Discontinuities and groundwater conditions are not considered in the analysis; including these would improve the reliability.
- Only UCS values from the laboratory test of the rock sample were available and used in the numerical analysis; conducting laboratory tests for additional parameters (e.g., Young's modulus, Poisson's ratio) could refine the outcomes.

7 REFERENCES

1. Akdag, S., Karakus, M., Nguyen, G., & Taheri, A. (2017). *Influence of specimen dimensions on bursting behavior of rocks under true triaxial loading condition*. 447–457.

2. Dietz, T., Auffenberg, J., Estrella Chong, A., Grabs, J., & Kilian, B. (2018). The Voluntary Coffee Standard Index (VOCSI). Developing a Composite Index to Assess and Compare the Strength of Mainstream Voluntary Sustainability Standards in the Global Coffee Industry. *Ecological Economics*, *150*, 72–87.

3. Dowding, C. H., & Andersson, C.-A. (1986). Potential for rock bursting and slabbing in deep caverns. *Engineering Geology*, *22*(3), 265–279.

4. Fukui, K., Okubo, S., & Ogawa, A. (2004). Some aspects of loading-rate dependency of Sanjome andesite strengths. *International Journal of Rock Mechanics and Mining Sciences*, *41*(7), 1215–1219.

5. Gong, F., & Li, X. (2007). A distance discriminant analysis method for prediction of possibility and classification of rockburst and its application. *Chinese Journal of Rock Mechanics and Engineering*, *26*.

6. Hoek, E. (2001). Big Tunnels in Bad Rock. *Journal of Geotechnical and Geoenvironmental Engineering*, *127*(9), 726–740.

7. Hoek, E., & Brown, E. T. (1980a). Empirical Strength Criterion for Rock Masses. *Journal of the Geotechnical Engineering Division*, *106*(9), 1013–1035.

8. Hoek, E., & Brown, E. T. (1980b). Empirical Strength Criterion for Rock Masses. *Journal of the Geotechnical Engineering Division*, *106*(9), 1013–1035.

9. Li, T., Ma, C., Zhu, M., Meng, L., & Chen, G. (2017). Geomechanical types and mechanical analyses of rockbursts. *Engineering Geology*, *222*, 72–83.

10. Ortlepp, W. D., & Stacey, T. R. (1994). Rockburst mechanisms in tunnels and shafts. *Tunnelling and Underground Space Technology*, *9*(1), 59–65.

11. Qin, C., Zhao, W., Chen, W., Zhang, X., & Xie, P. (2026). Prediction of rockburst risk induced by mine tremor using ensemble learning techniques. *Journal of Rock Mechanics and Geotechnical Engineering*, *18*(3), 1937–1953.

12. Shrestha, G. L., & Broch, E. (2008). Influences of the valley morphology and rock mass strength on tunnel convergence: With a case study of Khimti 1 headrace tunnel in Nepal. *Tunnelling and Underground Space Technology*, *23*(6), 638–650.

13. Singh, S. P. (1987). The influence of rock properties on the occurrence and control of rockbursts. *Mining Science and Technology*, *5*(1), 11–18.

14. Zhou, C., Dong, Z., Zhou, C., Fu, P., & Luo, S. (2024). Mechanical mechanism analysis of rockburst in deep-buried tunnel with high in-situ stress. *Scientific Reports*, *14*(1), 18076.

15. Zhuang, L., Zang, A., & Jung, S. (2022). Grain-scale analysis of fracture paths from high-cycle hydraulic fatigue experiments in granites and sandstone. *International Journal of Rock Mechanics and Mining Sciences*, *157*, 105177.

16. W. D. Ortlepp and T. R. Stacey, “Rock burst mechanisms in tunnels and shafts,” Tunnelling and Underground Space Technology, vol. 9, no. 1, pp. 59–65, Jan. 1994

17. S. P. Singh, “The influence of rock properties on the occurrence and control of rock bursts,” Mining Science and Technology, vol. 5, no. 1, pp. 11–18, May 1987

18. K. Fukui, S. Okubo, and A. Ogawa, “Some aspects of loading-rate dependency of Sanjome andesite strengths,” International Journal of Rock Mechanics and Mining Sciences, vol. 41, no. 7, pp. 1215–1219, Oct. 2004

19. L. Zhuang, A. Zang, and S. Jung, “Grain-scale analysis of fracture paths from high-cycle hydraulic fatigue experiments in granites and sandstone,” International Journal of Rock Mechanics and Mining Sciences, vol. 157, p. 105177, Sep. 2022

20. T. Li, C. Ma, M. Zhu, L. Meng, and G. Chen, “Geomechanical types and mechanical analyses of rock bursts,” Engineering Geology, vol. 222, pp. 72–83, May 2017.

21. S. Akdag, M. Karakus, G. Nguyen, and A. Taheri, “Influence of specimen dimensions on bursting behavior of rocks under true triaxial loading condition,” presented at the Eighth International Conference on Deep and High Stress Mining, 2017, pp. 447–457.

ANNEX-I: CONSENT APPROVAL

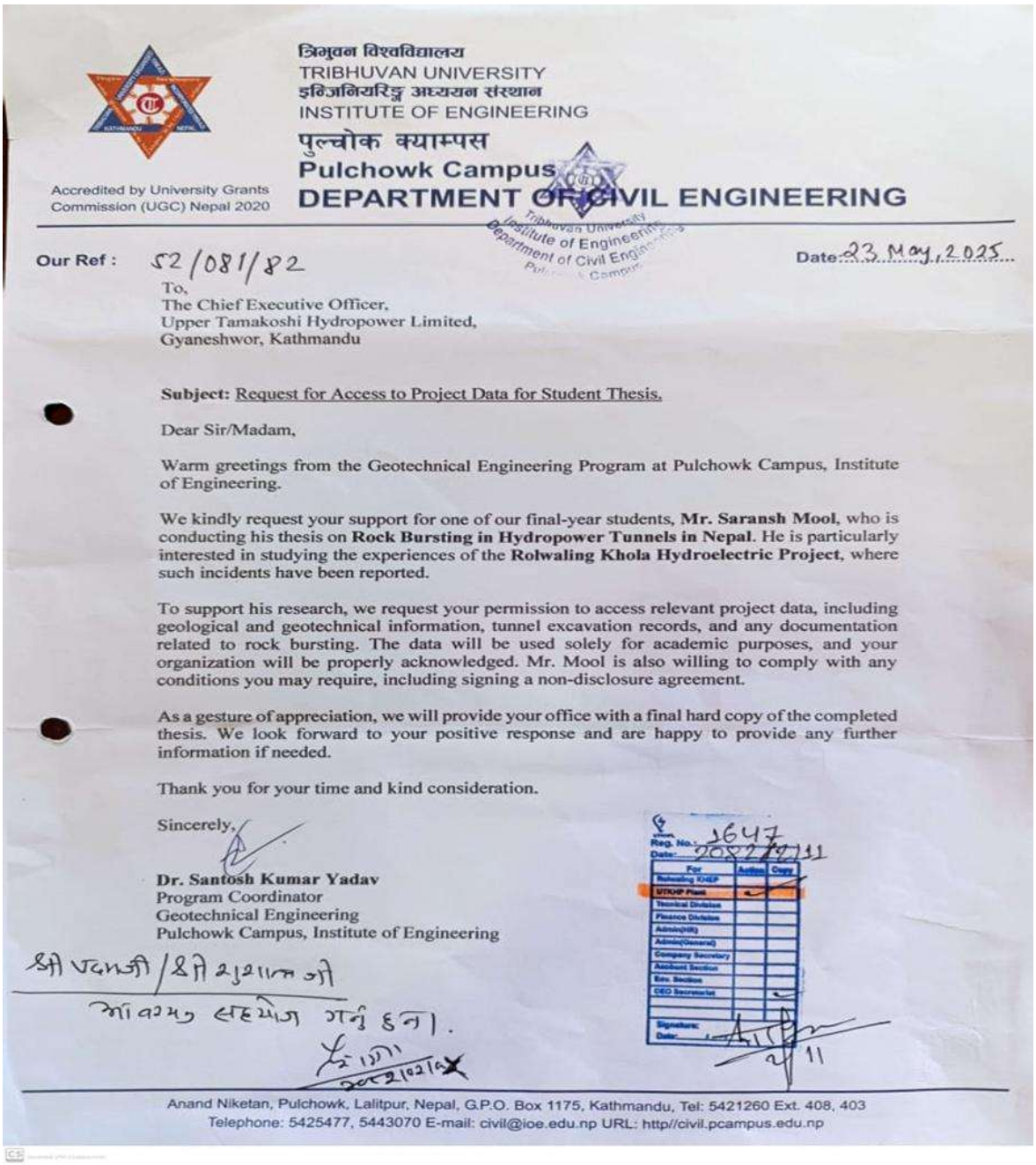

त्रिभुवन विश्वविद्यालय
TRIBHUVAN UNIVERSITY
इन्जिनियरिङ्ग अध्ययन संस्थान
INSTITUTE OF ENGINEERING
पुल्चोक क्याम्पस
Pulchowk Campus
DEPARTMENT OF CIVIL ENGINEERING

Accredited by University Grants Commission (UGC) Nepal 2020

Tribhuvan University Institute of Engineering Department of Civil Engineering Pulchowk Campus

Our Ref : 52/081/82

Date: 23 May, 2025

To,
The Chief Executive Officer,
Upper Tamakoshi Hydropower Limited,
Gyaneshwor, Kathmandu

Subject: Request for Access to Project Data for Student Thesis.

Dear Sir/Madam,

Warm greetings from the Geotechnical Engineering Program at Pulchowk Campus, Institute of Engineering.

We kindly request your support for one of our final-year students, **Mr. Saransh Mool**, who is conducting his thesis on **Rock Bursting in Hydropower Tunnels in Nepal**. He is particularly interested in studying the experiences of the **Rolwaling Khola Hydroelectric Project**, where such incidents have been reported.

To support his research, we request your permission to access relevant project data, including geological and geotechnical information, tunnel excavation records, and any documentation related to rock bursting. The data will be used solely for academic purposes, and your organization will be properly acknowledged. Mr. Mool is also willing to comply with any conditions you may require, including signing a non-disclosure agreement.

As a gesture of appreciation, we will provide your office with a final hard copy of the completed thesis. We look forward to your positive response and are happy to provide any further information if needed.

Thank you for your time and kind consideration.

Sincerely,

Dr. Santosh Kumar Yadav
Program Coordinator
Geotechnical Engineering
Pulchowk Campus, Institute of Engineering

Reg. No.: 1647
Date: 2082/02/11

For	Action	Copy
Rolwaling KHEP		
UTKHP Plant	✓	
Technical Division		
Finance Division		
Admin(HR)		
Admin(General)		
Company Secretary		
Antikant Section		
Env. Section		
CEO Secretariat		✓
Signature: Date:		

श्री पदमजी / श्री उपाध्याय जी
आवश्यक सहयोग गर्नु हुन।

2082/02/11

Anand Niketan, Pulchowk, Lalitpur, Nepal, G.P.O. Box 1175, Kathmandu, Tel: 5421260 Ext. 408, 403
Telephone: 5425477, 5443070 E-mail: civil@ioe.edu.np URL: http//civil.pcampus.edu.np

ANNEX-II: ROCK BURST PHOTOGRAPHS

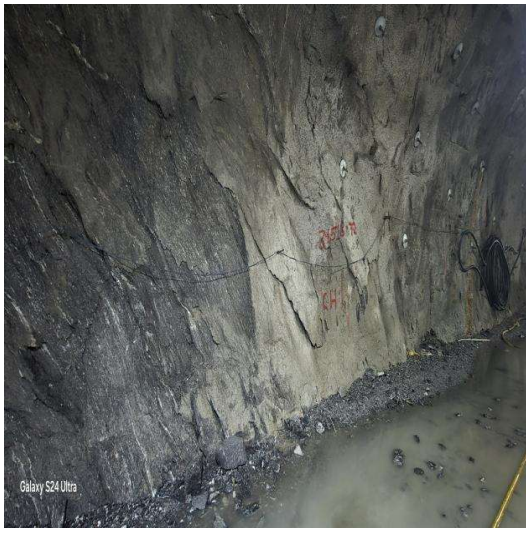

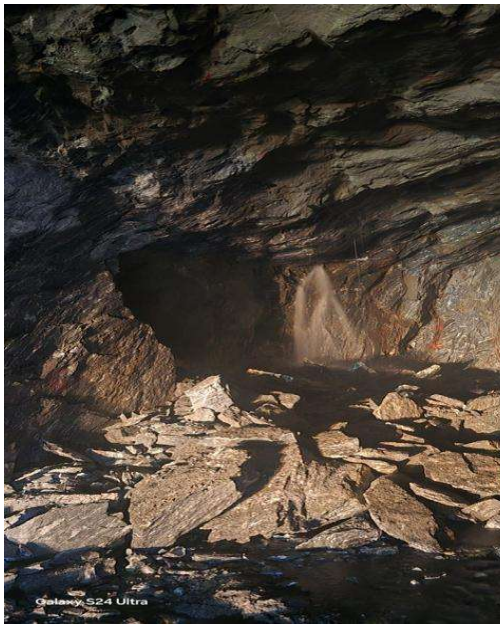

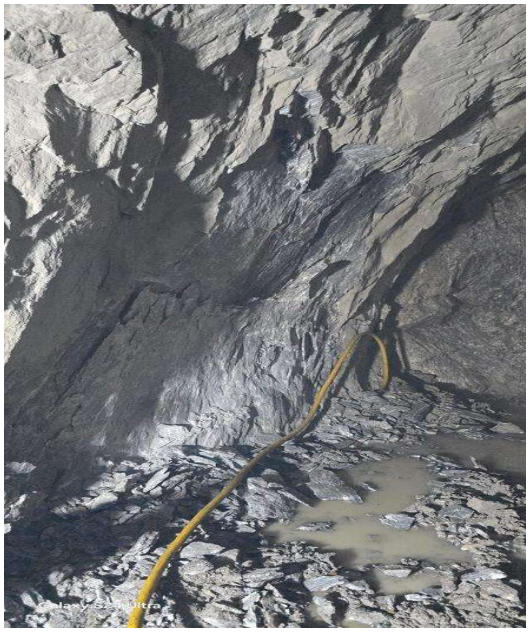

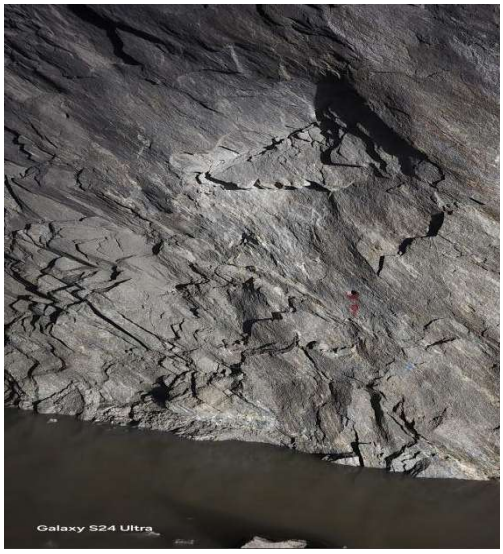
Galaxy S24 Ultra

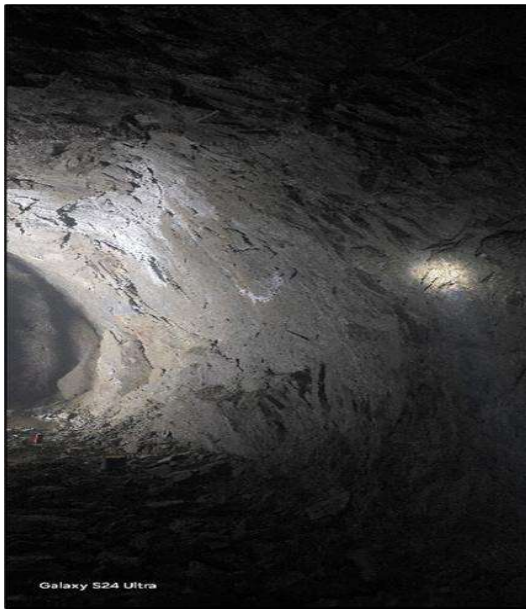
Galaxy S24 Ultra

ANNEX-III: WATER SEEPAGE MEASUREMENT

EPC CONSTRUCTION OF ROLWALING KHOLA HYDROELECTRIC PROJECT (22.00MW)
(CONTRACT IDENTIFICATION NO. RKHEP/ICB/02/2076/77)
Measurement of Groundwater in the Headrace Tunnel

Date: 2081/12/27

SN	Chainage	Location	Amount of flow (lit)	Time Taken (sec)	Flow (lit/sec)	Flow (lit/min)	Remarks
1	3+593.71	left SPL	5	74	0.068	4.05	
2	3+604.71	Right SPL	5	34	0.147	8.82	
3	3+610.71	Right SPL	5	99	0.051	3.03	
4	3+642.71	Right Crown	5	86	0.058	3.49	
5	3+654.11	Right SPL	10	12	0.833	50.00	
6	3+656.11	Right SPL	10	63	0.159	9.52	
7	3+658.71	Right Crown	5	10	0.500	30.00	
8	3+659.11	Right SPL	10	73	0.137	8.22	
9	3+660.51	Right SPL	5	50	0.100	6.00	
10	3+665.61	Right SPL	5	80	0.063	3.75	
11	3+671.71	Center Crown	5	23	0.217	13.04	
12	3+681.71	Right Crown	5	56	0.089	5.36	
13	3+689.71	Right Crown	5	54	0.093	5.56	
14	3+690.71	Right Crown	5	64	0.078	4.69	
15	3+699.71	Right SPL	5	33	0.152	9.09	
16	3+713.21	Right SPL	5	26	0.192	11.54	
17	3+713.36	Left SPL	5	105	0.048	2.86	
18	3+719.21	Left Crown	5	16	0.313	18.75	
19	3+722.21	Center Crown	5	9	0.556	33.33	
20	3+736.71	Right SPL	5	130	0.038	2.31	
21	3+886.00	Right Crown	5	100	0.050	3.00	
22	3+890.00	Right SPL	5	146	0.034	2.05	
23	3+892.00	Center Crown	5	82	0.061	3.66	
24	3+921.00	Left SPL	3	108	0.028	1.67	
25	3+923.00	Right SPL	2	110	0.018	1.09	
26	3+950.00	Left SPL	5	230	0.022	1.30	
27	3+952.00	Right SPL	5	29	0.172	10.34	
28	3+958.00	Left SPL	5	50	0.100	6.00	
29	3+958.00	Left SPL	2.5	73	0.034	2.05	
30	3+960.00	Left SPL	5	5	1.000	60.00	
31	4+014.71	Left Crown	5	16	0.313	18.75	
32	4+203.00	Right Crown	5	57	0.088	5.26	
33	4+209.00	Crown	5	160	0.031	1.88	

EPC CONSTRUCTION OF ROLWALING KHOLA HYDROELECTRIC PROJECT (22.00MW)
(CONTRACT IDENTIFICATION NO. RKHEP/ICB/02/2076/77)

Measurement of Groundwater in the Headrace Tunnel

Date: 2081/12/27

SN	Chainage	Location	Amount of flow (lit)	Time Taken (sec)	Flow (lit/sec)	Flow (lit/min)	Remarks
1	3+593.71	left SPL	5	74	0.068	4.05	
2	3+604.71	Right SPL	5	34	0.147	8.82	
3	3+610.71	Right SPL	5	99	0.051	3.03	
4	3+642.71	Right Crown	5	86	0.058	3.49	
5	3+654.11	Right SPL	10	12	0.833	50.00	
6	3+656.11	Right SPL	10	63	0.159	9.52	
7	3+658.71	Right Crown	5	10	0.500	30.00	
8	3+659.11	Right SPL	10	73	0.137	8.22	
9	3+660.51	Right SPL	5	50	0.100	6.00	
10	3+665.61	Right SPL	5	80	0.063	3.75	
11	3+671.71	Center Crown	5	23	0.217	13.04	
12	3+681.71	Right Crown	5	56	0.089	5.36	
13	3+689.71	Right Crown	5	54	0.093	5.56	
14	3+690.71	Right Crown	5	64	0.078	4.69	
15	3+699.71	Right SPL	5	33	0.152	9.09	
16	3+713.21	Right SPL	5	26	0.192	11.54	
17	3+713.36	Left SPL	5	105	0.048	2.86	
18	3+719.21	Left Crown	5	16	0.313	18.75	
19	3+722.21	Center Crown	5	9	0.556	33.33	
20	3+736.71	Right SPL	5	130	0.038	2.31	
21	3+886.00	Right Crown	5	100	0.050	3.00	
22	3+890.00	Right SPL	5	146	0.034	2.05	
23	3+892.00	Center Crown	5	82	0.061	3.66	
24	3+921.00	Left SPL	3	108	0.028	1.67	
25	3+923.00	Right SPL	2	110	0.018	1.09	
26	3+950.00	Left SPL	5	230	0.022	1.30	
27	3+952.00	Right SPL	5	29	0.172	10.34	
28	3+958.00	Left SPL	5	50	0.100	6.00	
29	3+958.00	Left SPL	2.5	73	0.034	2.05	
30	3+960.00	Left SPL	5	5	1.000	60.00	
31	4+014.71	Left Crown	5	16	0.313	18.75	
32	4+203.00	Right Crown	5	57	0.088	5.26	
33	4+209.00	Crown	5	160	0.031	1.88	

ANNEX-IV: GEOLOGICAL FACEMAP

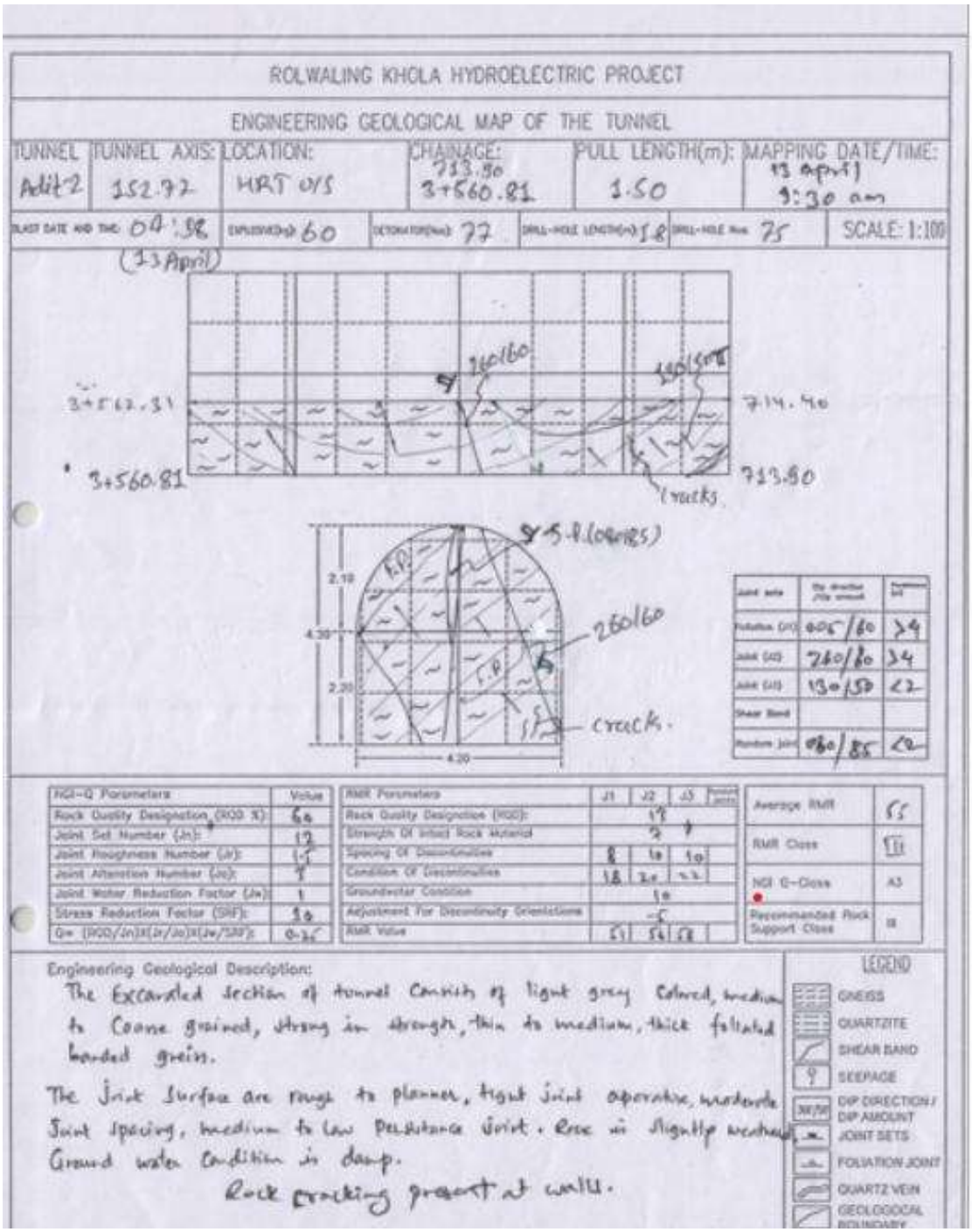

ROLWALING KHOLA HYDROELECTRIC PROJECT

ENGINEERING GEOLOGICAL MAP OF THE TUNNEL

TUNNEL	TUNNEL AXIS:	LOCATION:	CHAINAGE:	PULL LENGTH(m):	MAPPING DATE/TIME:
Adit 2	152.72	HRT O/S	713.90 3+560.81	1.50	13 April 9:30 am

BLAST DATE AND TIME:	EXPLOSIVES(kg):	DETONATOR(Nos):	DRILL-HOLE LENGTH(m):	DRILL-HOLE Nos:	SCALE: 1:100
04:38	60	77	1.8	75	

(13 April)

3+562.31 — 714.40 — 3+560.81 — 713.90

260/60 — 140/50 — rocks

2.10 — 4.20 — 2.30 — 4.20

260/60 — creack.

Joint sets	Dip direction/Dip amount	Persistence (m)
Foliation (J1)	005/60	>4
Joint (J2)	260/80	>4
Joint (J3)	130/50	<2
Shear Band		
Random Joint	080/85	<2

NGI-Q Parameters	Value
Rock Quality Designation (RQD %):	60
Joint Set Number (Jn):	12
Joint Roughness Number (Jr):	1.5
Joint Alteration Number (Ja):	4
Joint Water Reduction Factor (Jw):	1
Stress Reduction Factor (SRF):	10
Q= (RQD/Jn)x(Jr/Ja)x(Jw/SRF):	0.75

RMR Parameters	J1	J2	J3	Remarks
Rock Quality Designation (RQD):	17			
Strength Of Intact Rock Material	2			
Spacing Of Discontinuities	8	10	10	
Condition Of Discontinuities	18	20	22	
Groundwater Condition	10			
Adjustment For Discontinuity Orientations	-5			
RMR Value	51	54	52	

Average RMR	55
RMR Class	III
NGI Q-Class	A3
Recommended Rock Support Class	III

Engineering Geological Description:

The Excavated section of tunnel Consists of light grey Colored, medium to Coarse grained, strong in strength, thin to medium, thick foliated banded gneiss.

The Joint Surface are rough to planner, tight Joint operative, moderate Joint Spacing, medium to Low Persistance Joint. Rock is Slightly weather. Ground water Condition is damp.

Rock cracking present at walls.

LEGEND

- GNEISS
- QUARTZITE
- SHEAR BAND
- SEEPAGE
- DIP DIRECTION / DIP AMOUNT
- JOINT SETS
- FOLIATION JOINT
- QUARTZ VEIN
- GEOLOGOCAL BOUNDARY

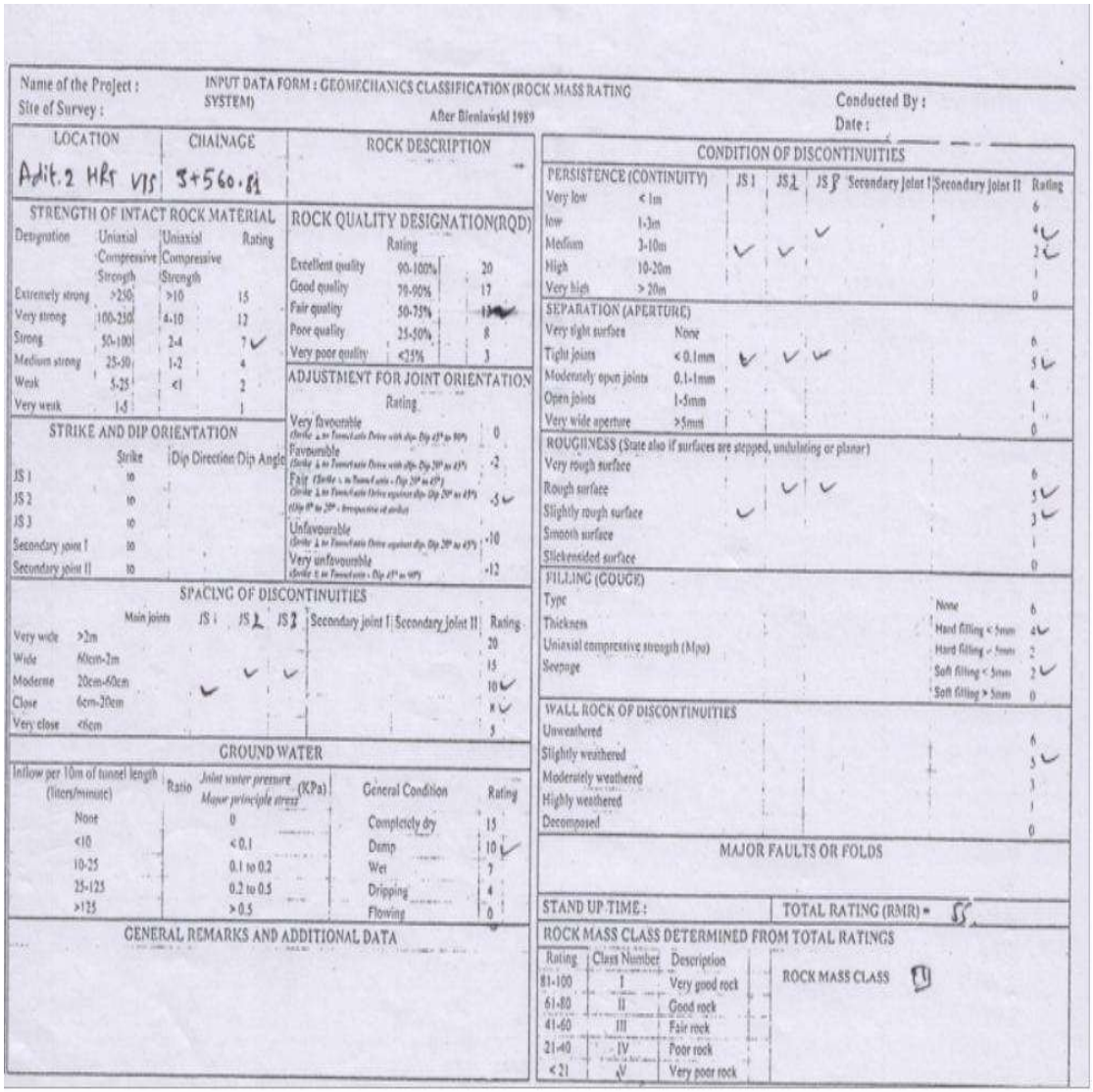

Name of the Project :
Site of Survey :

INPUT DATA FORM : GEOMECHANICS CLASSIFICATION (ROCK MASS RATING SYSTEM)
After Bieniawski 1989

Conducted By :
Date :

LOCATION	CHAINAGE	ROCK DESCRIPTION
Adit.2 HRT VIS	3+560.81	

STRENGTH OF INTACT ROCK MATERIAL

Designation	Uniaxial Compressive Strength	Uniaxial Compressive Strength	Rating
Extremely strong	>250	>10	15
Very strong	100-250	4-10	12
Strong	50-100	2-4	7 ✓
Medium strong	25-50	1-2	4
Weak	5-25	<1	2
Very weak	1-5		1

ROCK QUALITY DESIGNATION(RQD)

Rating		
Excellent quality	90-100%	20
Good quality	75-90%	17
Fair quality	50-75%	13
Poor quality	25-50%	8
Very poor quality	<25%	3

STRIKE AND DIP ORIENTATION

	Strike	Dip Direction	Dip Angle
JS 1	to		
JS 2	to		
JS 3	to		
Secondary joint I	to		
Secondary joint II	to		

ADJUSTMENT FOR JOINT ORIENTATION

Rating	
Very favourable	0
Favourable	-2
Fair	-5 ✓
Unfavourable	-10
Very unfavourable	-12

SPACING OF DISCONTINUITIES

	Main joints	JS 1	JS 2	JS 3	Secondary joint I	Secondary joint II	Rating
Very wide	>2m						20
Wide	60cm-2m						15
Moderate	20cm-60cm		✓	✓			10 ✓
Close	6cm-20cm	✓					8 ✓
Very close	<6cm						5

GROUND WATER

Inflow per 10m of tunnel length (liters/minute)	Ratio Joint water pressure / Major principle stress	(KPa)	General Condition	Rating
None	0		Completely dry	15
<10	<0.1		Damp	10 ✓
10-25	0.1 to 0.2		Wet	7
25-125	0.2 to 0.5		Dripping	4
>125	>0.5		Flowing	0

GENERAL REMARKS AND ADDITIONAL DATA

CONDITION OF DISCONTINUITIES

PERSISTENCE (CONTINUITY)		JS 1	JS 2	JS 3	Secondary Joint I	Secondary Joint II	Rating
Very low	< 1m						6
low	1-3m			✓			4 ✓
Medium	3-10m	✓	✓				2 ✓
High	10-20m						1
Very high	> 20m						0

SEPARATION (APERTURE)							
Very tight surface	None						6
Tight joints	< 0.1mm	✓	✓	✓			5 ✓
Moderately open joints	0.1-1mm						4
Open joints	1-5mm						1
Very wide aperture	>5mm						0

ROUGHNESS (State also if surfaces are stepped, undulating or planar)							
Very rough surface							6
Rough surface			✓	✓			5 ✓
Slightly rough surface		✓					3 ✓
Smooth surface							1
Slickensided surface							0

FILLING (GOUGE)		
Type	None	6
Thickness	Hard filling < 5mm	4 ✓
Uniaxial compressive strength (Mpa)	Hard filling > 5mm	2
Seepage	Soft filling < 5mm	2 ✓
	Soft filling > 5mm	0

WALL ROCK OF DISCONTINUITIES	
Unweathered	6
Slightly weathered	5 ✓
Moderately weathered	3
Highly weathered	1
Decomposed	0

MAJOR FAULTS OR FOLDS

STAND UP TIME :

TOTAL RATING (RMR) = 55

ROCK MASS CLASS DETERMINED FROM TOTAL RATINGS

Rating	Class Number	Description
81-100	I	Very good rock
61-80	II	Good rock
41-60	III	Fair rock
21-40	IV	Poor rock
< 21	V	Very poor rock

ROCK MASS CLASS III

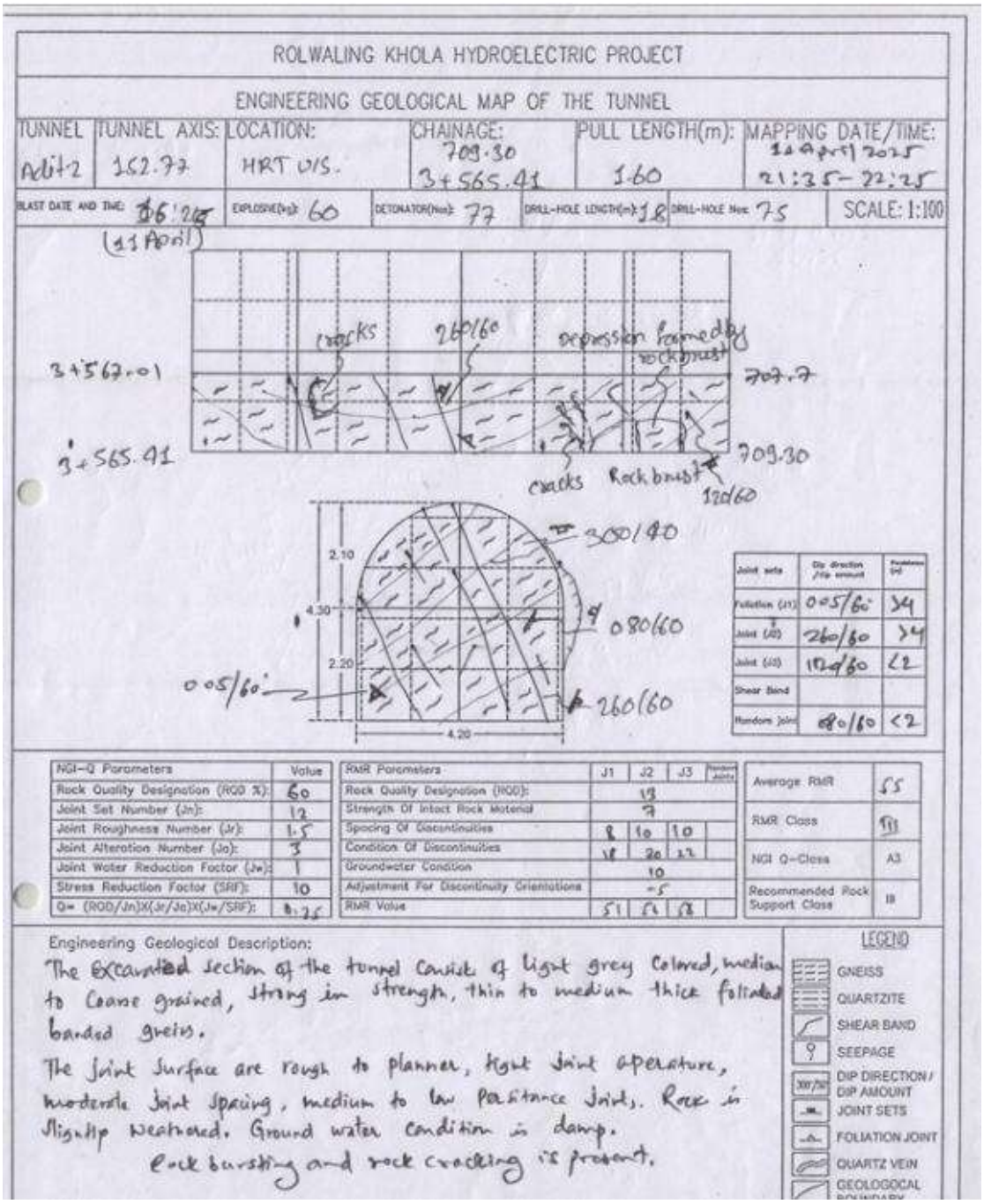

ROLWALING KHOLA HYDROELECTRIC PROJECT

ENGINEERING GEOLOGICAL MAP OF THE TUNNEL

TUNNEL	TUNNEL AXIS:	LOCATION:	CHAINAGE:	PULL LENGTH(m):	MAPPING DATE/TIME:
Adit-2	152.77	HRT U/S.	709.30 3+565.41	1.60	10 April 2025 21:35 – 22:25

BLAST DATE AND TIME:	EXPLOSIVE(kg):	DETONATOR(Nos):	DRILL-HOLE LENGTH(m):	DRILL-HOLE Nos:	SCALE:
06:25 (11 April)	60	77	1.8	75	1:100

Joint sets	Dip direction / Dip amount	Persistence (m)
Foliation (J1)	005/60°	>4
Joint (J2)	260/60	>4
Joint (J3)	120/80	<2
Shear Band		
Random Joint	080/80	<2

NGI-Q Parameters	Value
Rock Quality Designation (RQD %):	60
Joint Set Number (Jn):	12
Joint Roughness Number (Jr):	1.5
Joint Alteration Number (Ja):	3
Joint Water Reduction Factor (Jw):	1
Stress Reduction Factor (SRF):	10
Q= (RQD/Jn)X(Jr/Ja)X(Jw/SRF):	0.25

RMR Parameters	J1	J2	J3	Random Joints
Rock Quality Designation (RQD):	13			
Strength Of Intact Rock Material	7			
Spacing Of Discontinuities	8	10	10	
Condition Of Discontinuities	12	20	22	
Groundwater Condition	10			
Adjustment For Discontinuity Orientations	-5			
RMR Value	51	54	58	

Average RMR	55
RMR Class	III
NGI Q-Class	A3
Recommended Rock Support Class	IB

Engineering Geological Description:

The excavated section of the tunnel consist of light grey colored, medium to coarse grained, strong in strength, thin to medium thick foliated banded gneiss.

The joint surface are rough to planner, tight joint aperature, moderate joint spacing, medium to low persistance joint. Rock is slightly weathered. Ground water condition is damp.

Rock bursting and rock cracking is present.

LEGEND

- GNEISS
- QUARTZITE
- SHEAR BAND
- SEEPAGE
- DIP DIRECTION / DIP AMOUNT
- JOINT SETS
- FOLIATION JOINT
- QUARTZ VEIN
- GEOLOGICAL BOUNDARY

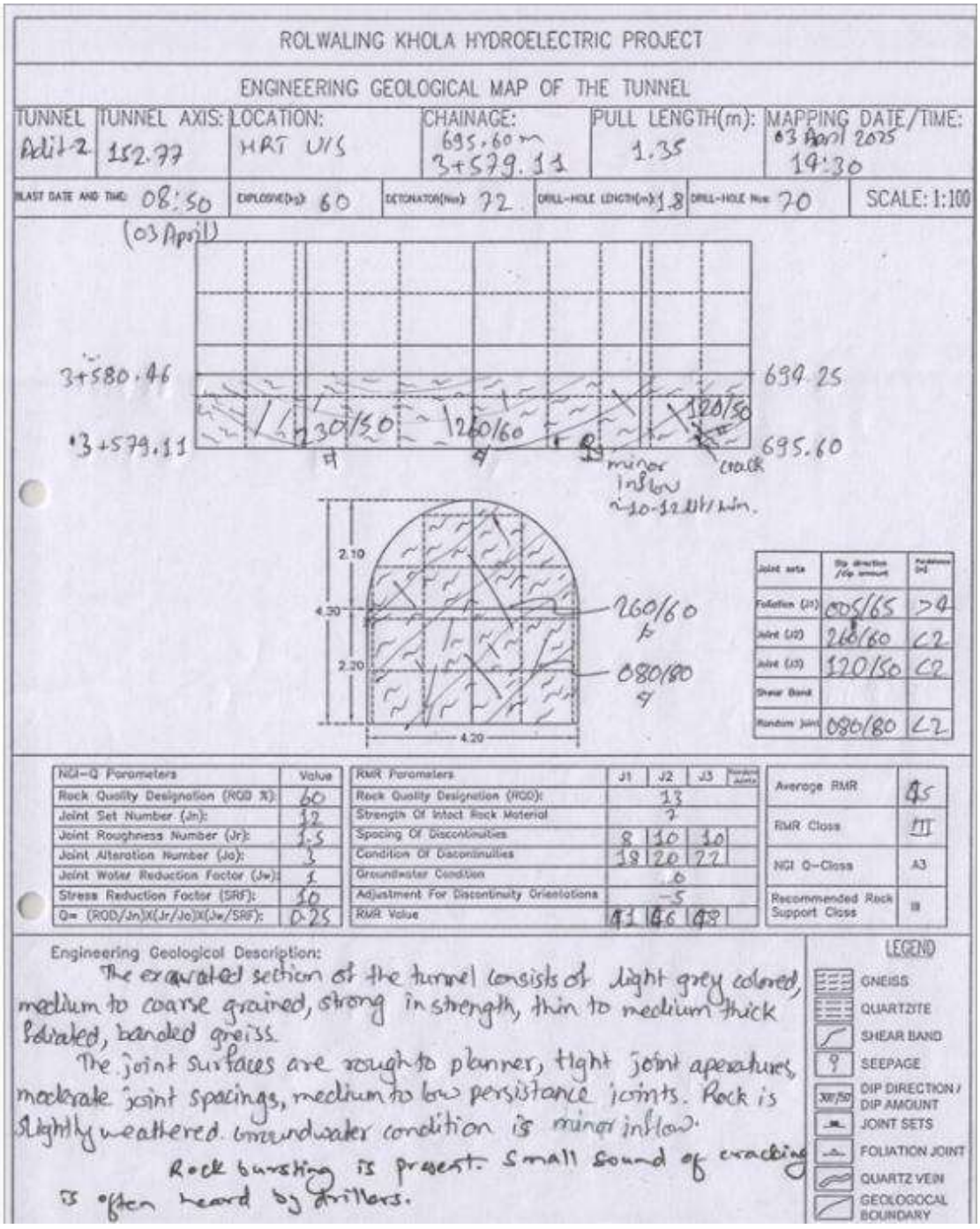

ROLWALING KHOLA HYDROELECTRIC PROJECT

ENGINEERING GEOLOGICAL MAP OF THE TUNNEL

TUNNEL	TUNNEL AXIS:	LOCATION:	CHAINAGE:	PULL LENGTH(m):	MAPPING DATE/TIME:
Adit-2	152.77	HRT U/S	695.60 m 3+579.11	1.35	03 April 2025 14:30

BLAST DATE AND TIME:	EXPLOSIVE(kg):	DETONATOR(Nos):	DRILL-HOLE LENGTH(m):	DRILL-HOLE Nos:	SCALE:
08:50	60	72	1.8	70	1:100

(03 April)

3+580.46

3+579.11

695.25

695.60

130/50

260/60

120/50

minor inflow ~10-12 lit/min.

crack

2.10

4.30

2.20

4.20

260/60

080/80

Joint sets	Dip direction / Dip amount	Persistence (m)
Foliation (J1)	005/65	>4
Joint (J2)	260/60	<2
Joint (J3)	120/50	<2
Shear Band		
Random Joint	080/80	<2

NGI-Q Parameters	Value
Rock Quality Designation (RQD %):	60
Joint Set Number (Jn):	12
Joint Roughness Number (Jr):	1.5
Joint Alteration Number (Ja):	3
Joint Water Reduction Factor (Jw):	1
Stress Reduction Factor (SRF):	10
Q= (RQD/Jn)X(Jr/Ja)X(Jw/SRF):	0.25

RMR Parameters	J1	J2	J3	Random Joints
Rock Quality Designation (RQD):	13			
Strength Of Intact Rock Material	7			
Spacing Of Discontinuities	8	10	10	
Condition Of Discontinuities	18	20	22	
Groundwater Condition	0			
Adjustment For Discontinuity Orientations	-5			
RMR Value	61	66	68	

Average RMR	65
RMR Class	III
NGI Q-Class	A3
Recommended Rock Support Class	III

Engineering Geological Description:

The excavated section of the tunnel consists of light grey colored, medium to coarse grained, strong in strength, thin to medium thick foliated, banded gneiss.

The joint surfaces are rough to planner, tight joint apertures, moderate joint spacings, medium to low persistance joints. Rock is slightly weathered. Groundwater condition is minor inflow.

Rock bursting is present. Small sound of cracking is often heard by drillers.

LEGEND

- GNEISS
- QUARTZITE
- SHEAR BAND
- SEEPAGE
- 30/50 DIP DIRECTION / DIP AMOUNT
- JOINT SETS
- FOLIATION JOINT
- QUARTZ VEIN
- GEOLOGOCAL BOUNDARY

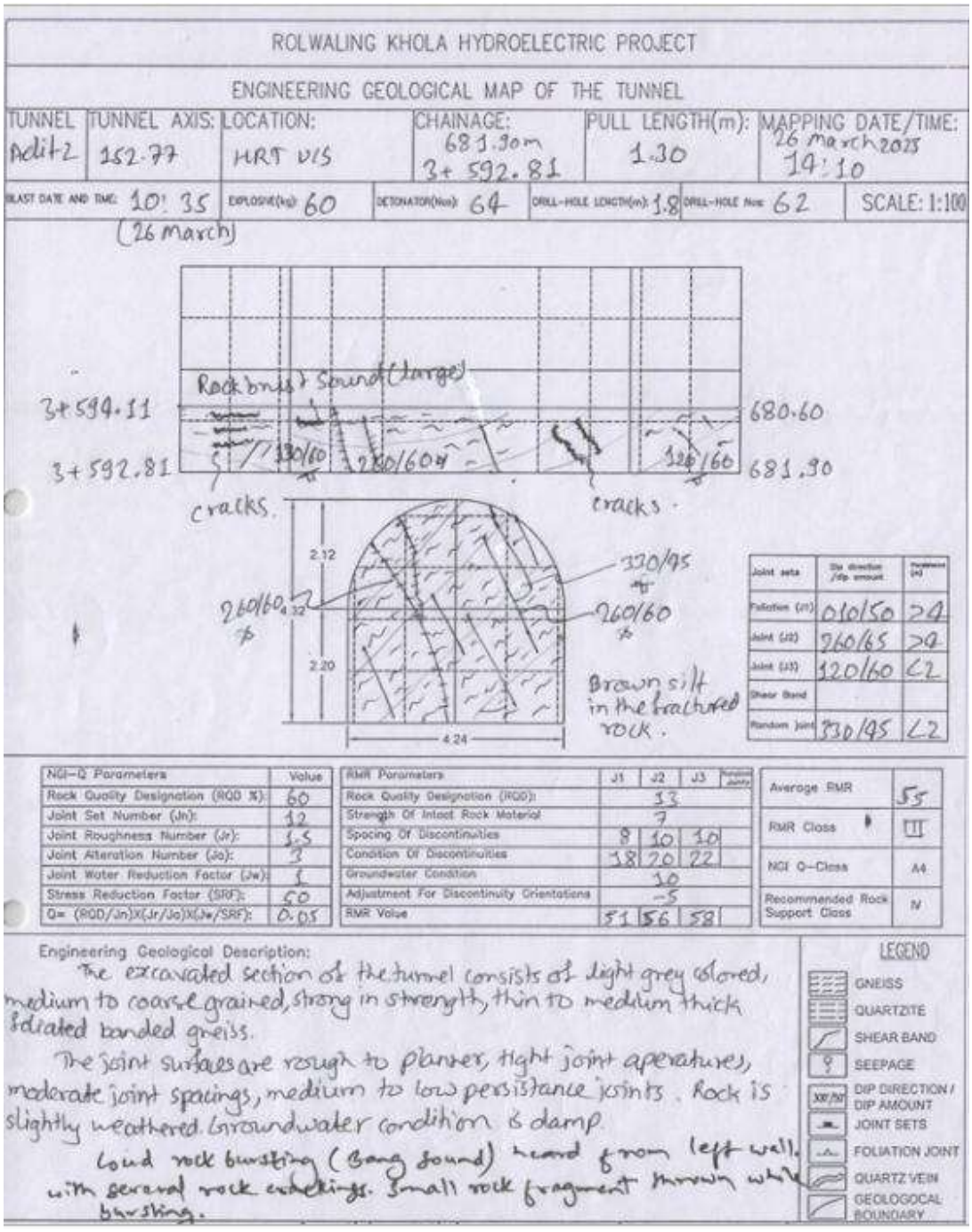

ROLWALING KHOLA HYDROELECTRIC PROJECT

ENGINEERING GEOLOGICAL MAP OF THE TUNNEL

TUNNEL	TUNNEL AXIS:	LOCATION:	CHAINAGE:	PULL LENGTH(m):	MAPPING DATE/TIME:
Adit-2	152.77	HRT U/S	681.90m 3+592.81	1.30	26 March 2025 14:10

BLAST DATE AND TIME:	EXPLOSIVE(kg):	DETONATOR(Nos):	DRILL-HOLE LENGTH(m):	DRILL-HOLE Nos:	SCALE: 1:100
10:35 (26 March)	60	64	1.8	62	

Rock burst + Sound (large)

3+594.11 — 680.60

3+592.81 — 681.90

330/60 — 320/60 — 320/60

cracks. — cracks.

2.12 — 2.32 — 2.20 — 4.24

260/60 — 330/95 — 260/60

Brown silt in the fractured rock.

Joint sets	Dip direction /dip amount	Persistence (m)
Foliation (J1)	010/50	>4
Joint (J2)	260/65	>4
Joint (J3)	320/60	<2
Shear Band		
Random Joint	330/95	<2

NGI-Q Parameters	Value
Rock Quality Designation (RQD %):	60
Joint Set Number (Jn):	12
Joint Roughness Number (Jr):	1.5
Joint Alteration Number (Ja):	3
Joint Water Reduction Factor (Jw):	1
Stress Reduction Factor (SRF):	50
Q= (RQD/Jn)X(Jr/Ja)X(Jw/SRF):	0.05

RMR Parameters	J1	J2	J3	Random Joints
Rock Quality Designation (RQD):	13			
Strength Of Intact Rock Material	7			
Spacing Of Discontinuities	8	10	10	
Condition Of Discontinuities	18	20	22	
Groundwater Condition	10			
Adjustment For Discontinuity Orientations	-5			
RMR Value	51	56	58	

Average RMR	55
RMR Class	III
NGI Q-Class	A4
Recommended Rock Support Class	IV

Engineering Geological Description:

The excavated section of the tunnel consists of light grey colored, medium to coarse grained, strong in strength, thin to medium thick foliated banded gneiss.

The joint surfaces are rough to planer, tight joint aperatures, moderate joint spacings, medium to low persistance joints. Rock is slightly weathered. Groundwater condition is damp.

Loud rock bursting (Bang sound) heard from left wall, with several rock cracklings. Small rock fragment thrown while bursting.

LEGEND

- GNEISS
- QUARTZITE
- SHEAR BAND
- SEEPAGE
- DIP DIRECTION / DIP AMOUNT
- JOINT SETS
- FOLIATION JOINT
- QUARTZ VEIN
- GEOLOGOCAL BOUNDARY

ANNEX-V: ROCK SUPPORT DRAWINGS

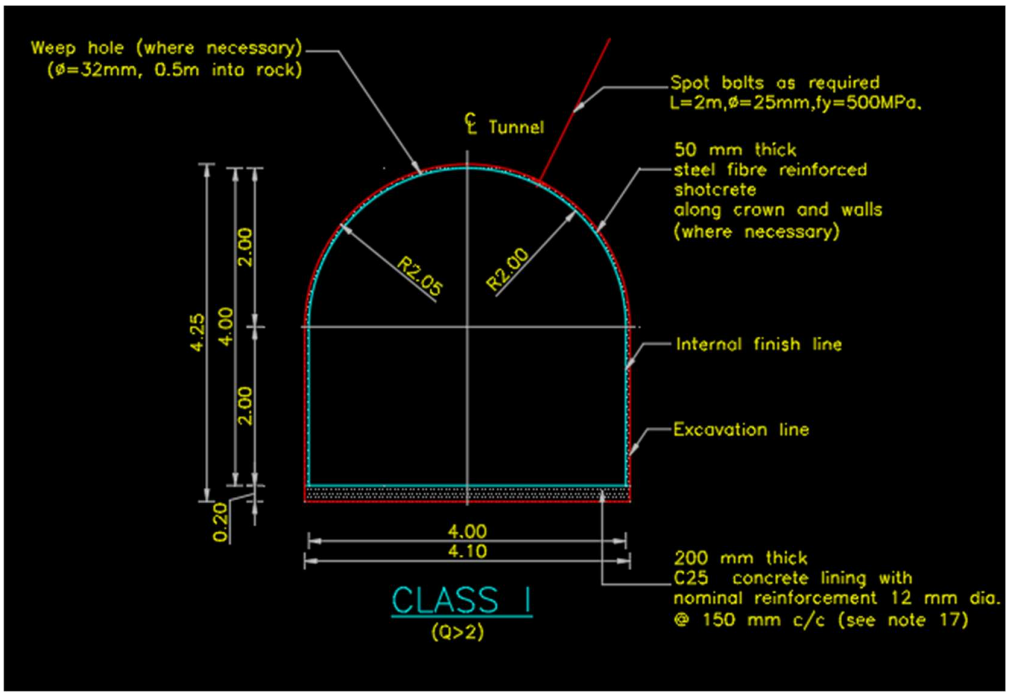

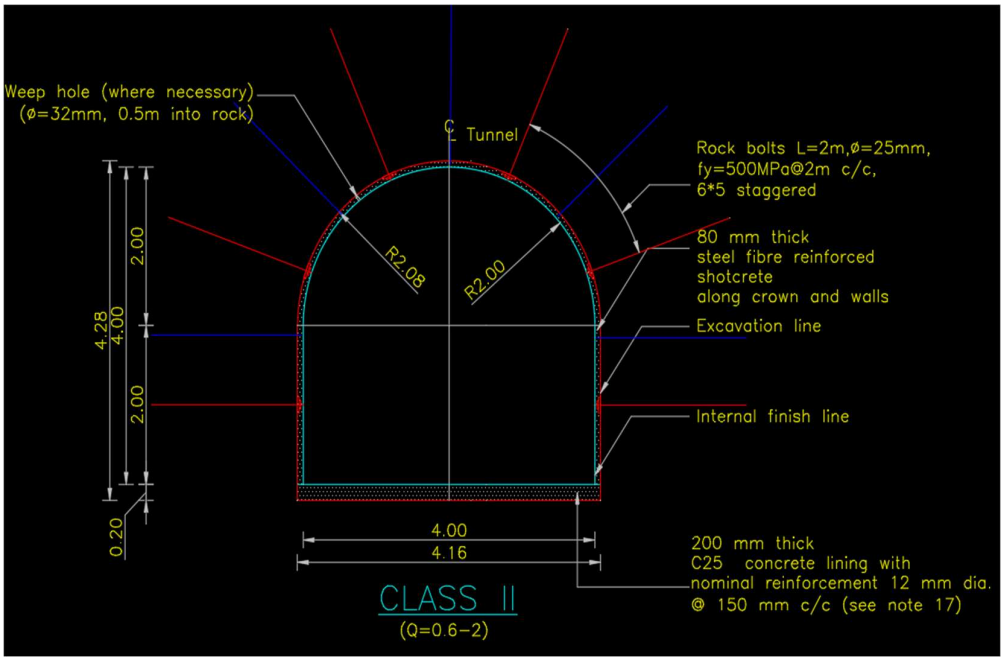

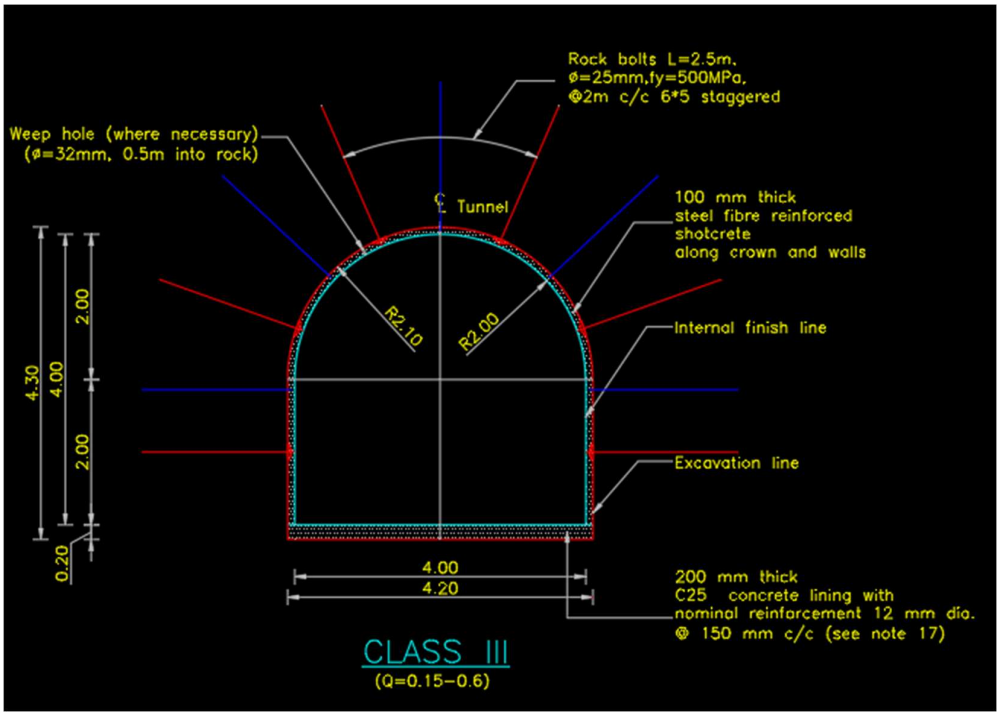
Rock bolts L=2.5m,
ø=25mm,fy=500MPa,
@2m c/c 6*5 staggered
Weep hole (where necessary)
(ø=32mm, 0.5m into rock)
℄ Tunnel
100 mm thick
steel fibre reinforced
shotcrete
along crown and walls
R2.10
R2.00
Internal finish line
Excavation line
4.30
4.00
2.00
2.00
0.20
4.00
4.20
200 mm thick
C25 concrete lining with
nominal reinforcement 12 mm dia.
@ 150 mm c/c (see note 17)
CLASS III
(Q=0.15-0.6)

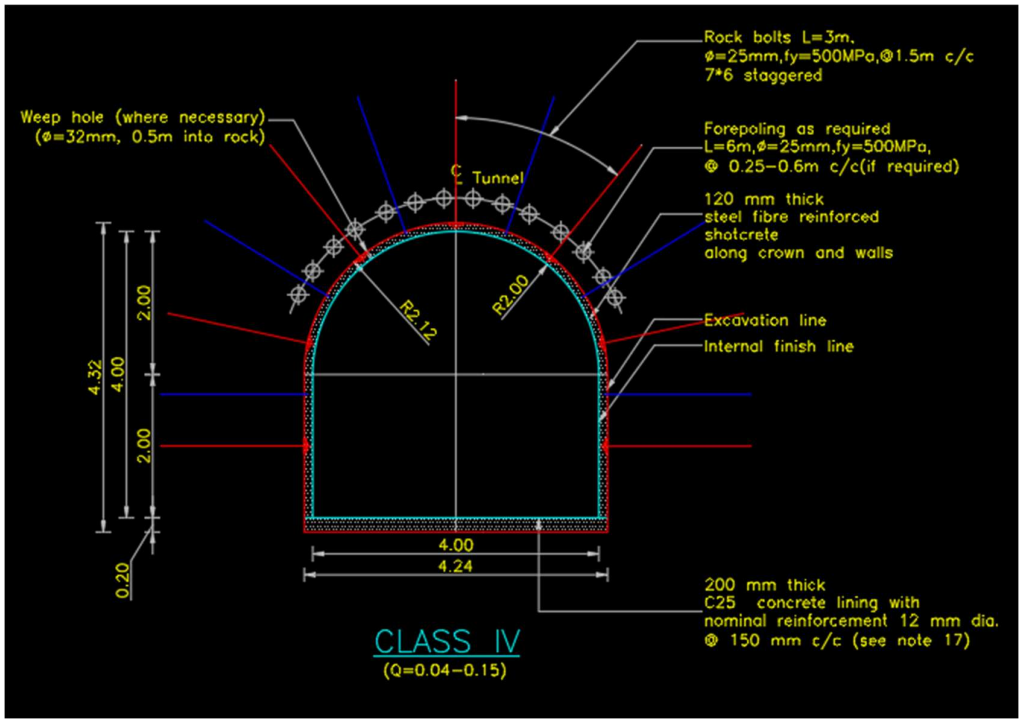
Rock bolts L=3m,
ø=25mm,fy=500MPa,@1.5m c/c
7*6 staggered
Weep hole (where necessary)
(ø=32mm, 0.5m into rock)
Forepoling as required
L=6m,ø=25mm,fy=500MPa,
@ 0.25-0.6m c/c(if required)
℄ Tunnel
120 mm thick
steel fibre reinforced
shotcrete
along crown and walls
R2.12
R2.00
Excavation line
Internal finish line
4.32
4.00
2.00
2.00
0.20
4.00
4.24
200 mm thick
C25 concrete lining with
nominal reinforcement 12 mm dia.
@ 150 mm c/c (see note 17)
CLASS IV
(Q=0.04-0.15)

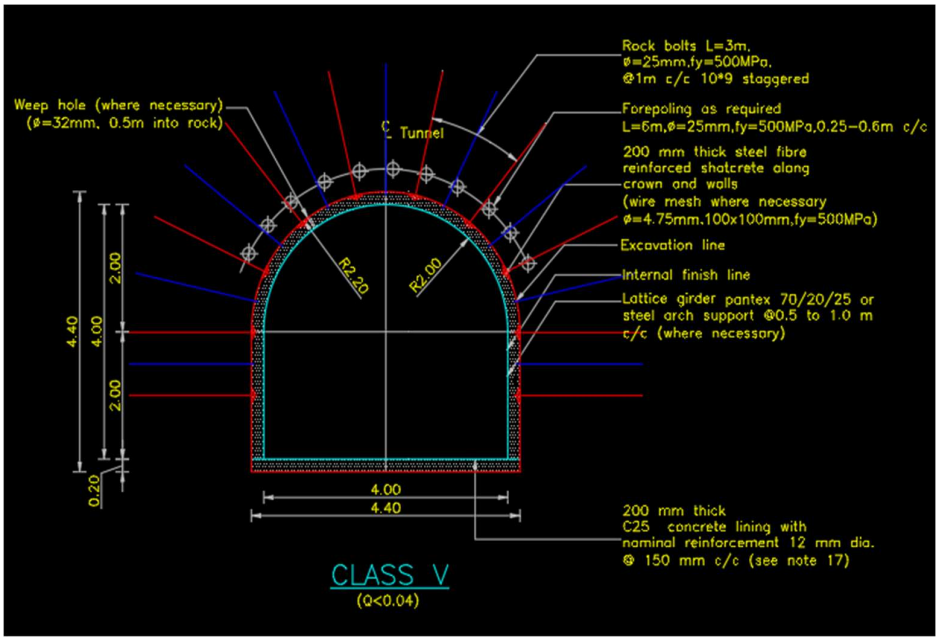
Rock bolts L=3m,
ø=25mm,fy=500MPa,
@1m c/c 10*9 staggered
Weep hole (where necessary)
(ø=32mm, 0.5m into rock)
℄ Tunnel
Forepoling as required
L=6m,ø=25mm,fy=500MPa,0.25-0.6m c/c
200 mm thick steel fibre
reinforced shotcrete along
crown and walls
(wire mesh where necessary
ø=4.75mm,100x100mm,fy=500MPa)
Excavation line
Internal finish line
Lattice girder pantex 70/20/25 or
steel arch support @0.5 to 1.0 m
c/c (where necessary)
R2.20
R2.00
4.40
4.00
2.00
2.00
0.20
4.00
4.40
200 mm thick
C25 concrete lining with
nominal reinforcement 12 mm dia.
@ 150 mm c/c (see note 17)
CLASS V
(Q<0.04)

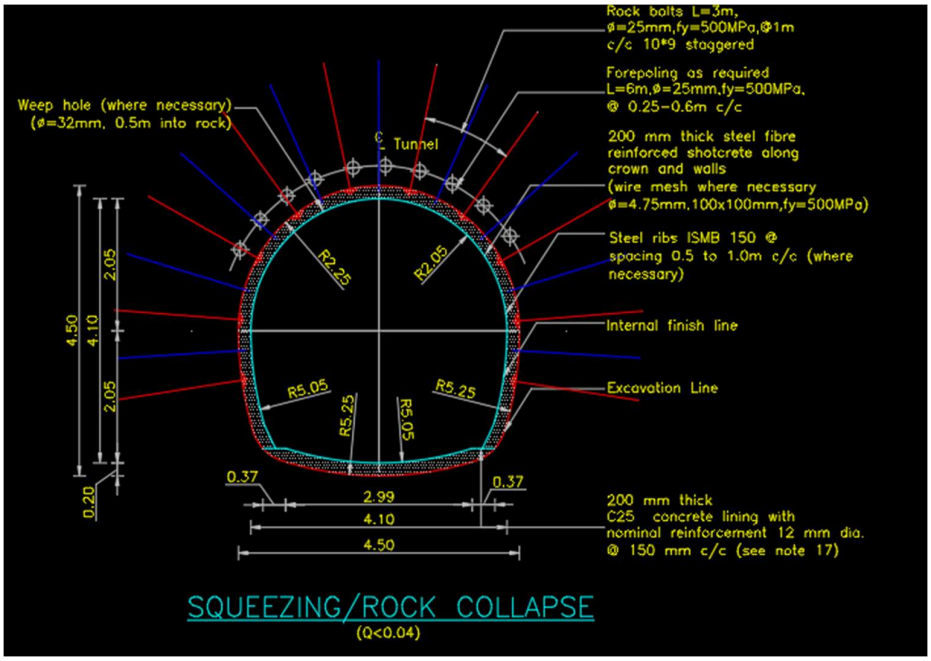
Rock bolts L=3m,
ø=25mm,fy=500MPa,@1m
c/c 10*9 staggered
Weep hole (where necessary)
(ø=32mm, 0.5m into rock)
Forepoling as required
L=6m,ø=25mm,fy=500MPa,
@ 0.25-0.6m c/c
℄ Tunnel
200 mm thick steel fibre
reinforced shotcrete along
crown and walls
(wire mesh where necessary
ø=4.75mm,100x100mm,fy=500MPa)
Steel ribs ISMB 150 @
spacing 0.5 to 1.0m c/c (where
necessary)
R2.25
R2.05
Internal finish line
Excavation Line
R5.05
R5.25
R5.25
R5.05
4.50
4.10
2.05
2.05
0.20
0.37
0.37
2.99
4.10
4.50
200 mm thick
C25 concrete lining with
nominal reinforcement 12 mm dia.
@ 150 mm c/c (see note 17)
SQUEEZING/ROCK COLLAPSE
(Q<0.04)